

Springer series in Physics

to be published.

# Ferroelectricity and Charge Ordering in Quasi One-Dimensional Organic Conductors

Serguei Brazovskii

LPTMS-CNRS, UMR8626, Univ. Paris Sud, bat 100, ORSAY CEDEX, F-91405  
and

L.D. Landau Institute for Theoretical Physics, Moscow, Russia

`brazov@lptms.u-psud.fr`

7 November 2006

## Abstract

The family of molecular conductors TMTTF/TMTSF-X demonstrates almost all known electronic phases in parallel with a set of weak structural modifications of ‘anion ordering’ and mysterious ‘structureless’ transitions. Only in early 2000s their nature became elucidated by discoveries of a huge anomaly in the dielectric permittivity and by the NMR evidences for the charge ordering (disproportionation). These observations have been interpreted as the never expected ferroelectric transition. The phenomenon unifies a variety of different concepts and observations in quite unusual aspects or conjunctions: ferroelectricity of good conductors, structural instability towards the Mott-Hubbard state, Wigner crystallization in a dense electronic system, the ordered  $4K_F$  charge density wave, richness of physics of solitons, interplay of structural and electronic symmetries. The corresponding theory of the “combined Mott-Hubbard state” deals with orthogonal contributions to the Umklapp scattering of electrons coming from the two symmetry breaking effects: the built-in nonequivalence of bonds and the spontaneous nonequivalence of sites. The state gives rise to several types of solitons, all of them showing in experiments. On this basis we can interpret the complex of existing experiments, and suggest future ones, such as optical absorption and photoconductivity, combined ferroelectric resonance and the phonon anti-resonance, plasma frequency reduction.

**keywords:** Organic conductors, ferroelectricity, charge ordering, charge disproportionation, solitons, optics, conductivity, permittivity.

Viewgraphs:  
<http://ipnweb.in2p3.fr/~lptms/membres/brazov/seminars.html>

# Contents

<b>1</b>	<b>Introduction. History and Events.</b>	<b>3</b>
<b>2</b>	<b>Hierarchy of phases in quasi 1D organic conductors.</b>	<b>5</b>
2.1	Structural transitions of the anion ordering. . . . .	6
2.2	Charge ordering transitions. . . . .	7
2.3	Overlapping and coexistence of phases. . . . .	9
2.4	Electronic mechanism of the charge ordering. . . . .	9
2.5	Electric polarization and Ferroelectricity. . . . .	11
<b>3</b>	<b>Electronic properties.</b>	<b>11</b>
3.1	Permittivity. . . . .	11
3.2	Conductivity. . . . .	12
<b>4</b>	<b>Ferroelectric Mott-Hubbard ground state.</b>	<b>15</b>
4.1	Choosing the theory approach. . . . .	15
4.2	Ground state and symmetry breaking. . . . .	16
<b>5</b>	<b>Elementary excitations.</b>	<b>18</b>
5.1	Solitons. . . . .	18
5.1.1	Solitons seen in most common cases. . . . .	18
5.1.2	Ferroelectric solitons. . . . .	19
5.2	Effects of subsequent transitions: Spin-charge reconfinement and combined solitons. . . . .	21
<b>6</b>	<b>Optics</b>	<b>22</b>
6.1	Optics: collective and mixed modes. . . . .	22
6.1.1	Optics: phase mode. . . . .	22
6.1.2	Optical permittivity $\varepsilon(\omega)$ near the ferroelectric transition. . . . .	23
6.2	Optics: solitons. . . . .	23
6.3	Optics: summary. . . . .	25
<b>7</b>	<b>Fate of the metallic TMTSF subfamily.</b>	<b>27</b>
<b>8</b>	<b>Origin and range of basic parameters.</b>	<b>28</b>
8.1	Generic origins of basic parameters: Interactions among electrons or with phonons? . . . . .	28
8.2	Where are we? . . . . .	29
<b>9</b>	<b>Conclusions and perspectives.</b>	<b>30</b>
<b>A</b>	<b>Earnshaw instability. Ion in the cage.</b>	<b>37</b>
<b>B</b>	<b>Permittivity sources.</b>	<b>38</b>
B.1	Estimations for the ionic contribution to $\varepsilon$ . . . . .	38
B.2	Phase instability. . . . .	39
<b>C</b>	<b>Competing philosophies for organic conductors.</b>	<b>39</b>
<b>D</b>	<b>History Excursions.</b>	<b>40</b>

# 1 Introduction. History and Events.

The discovery of first organic superconductors (Bechgaard, Jerome, Ribault, et al - 1979/80, see<sup>1</sup> [12, 13]) gave rise to a number of directions which none could foresee in advance. A great deal of experiments and theoretical speculations were done already within first years. Still a firework of phases was so amusingly rich that it feeds intensive research till our days. The twentieth anniversary was marked by a new discovery of Ferroelectricity and Charge Ordering/Disproportionation whose consequences are the subject of this review.

We shall address only quasi one-dimensional (1D) systems, and among them mostly the family of the Bechgaard-Fabre salts  $(\text{TMTCF})_2\text{X}$ , with extensions to related materials. Typically, the selenium subfamily  $(\text{TMTSF})_2\text{X}$  was a basis for research on the metallic phase: particularly the superconductivity and diverse spectacular magnetic oscillations. The sulphur subfamily  $(\text{TMTTF})_2\text{X}$  was suitable for effects of electronic correlations, particularly the Mott-Hubbard dielectrization. The studies were mostly concentrated upon electronic phase transitions, which take place between 1K and 20K, and on fashionable "non Fermi liquid" aspects of the normal state at higher T. Actually this "normal" part of the phase diagram was filled, for most of compositions X, with tiny structural transitions of "anion orderings" observed for all non-centrosymmetric counterions X ([14], and [15] for a review). Intentionally or not, these features were not appreciated either in experiments on electronic properties, or in theories - except notes by Emery [16] and a systematic approach of Yakovenko and the author [17, 18].

The most powerful sleeping bomb was hidden in mysterious "structureless transitions" registered in sulphur subfamily for centrosymmetric anions ( $\text{X}=\text{Br}$ ,  $\text{AsF}_6$ , etc.) at higher temperatures of about 100-250K ([19, 20, 21], and [22] for a recent review). Unexplained, unattended by the community and finally forgotten, these transitions have been waiting for a revenge since mid 80's. Only in 2000's their nature was identified, almost by chance, as something never expected: the ferroelectricity (FE) [23], or sometimes antiferroelectricity (AFE), see reviews [25, 26]. Moreover, the ferroelectricity happened to be a consequence of a hidden charge ordering/disproportionation (CO/CD) [27]<sup>2</sup>. The whole high temperature region of the phase diagram happened to be symmetry-broken. More history excursions can be found in [22, 28, 29], see also Appendix D.

The phenomenon is gaining ground, as it is being found in more and more compounds [22, 30, 31]. Also the charge ordering is registered now in layered organic materials, see [32, 33] for reviews, accompanied by the anomalously high dielectric permittivity [34], also signs of the ferroelectricity have been indicated [35]. The ferroelectricity was observed also in dielectric mixed-stacks organic compounds showing the neutral-ionic transition [36]. The energy scale (up to 300K in terms of temperatures and  $\sim 1000\text{K}$  in terms of energy gaps) of the charge ordering effect is so high that it allows to anticipate its hidden presence also in the metallic subfamily  $(\text{TMTSF})_2\text{X}$ ; the first direct sign has been brought by the case of  $(\text{TMTSF})_2\text{FSO}_3$  [33]. At least the effect must determine the properties of many materials where its presence has already been confirmed.

---

<sup>1</sup>We start the literature review with proceedings of most important scientific conferences and reviews collections [1, 2, 3, 4, 5, 6, 7, 8, 9, 10, 11].

<sup>2</sup>The terms Charge Ordering (CO), Charge Disproportionation (CD) and Charge Localization have been utilized in the literature to identify the described phenomena. Here we shall typically use a more easily pronounced version of charge ordering, and reserve the term charge disproportionation for the same effect to underline nonequal molecular charges. The charge ordering transition temperature will be called  $T_{\text{CO}}$ ; its other notations in the literature were typically  $T_0$  or  $T_{\text{CD}}$ .

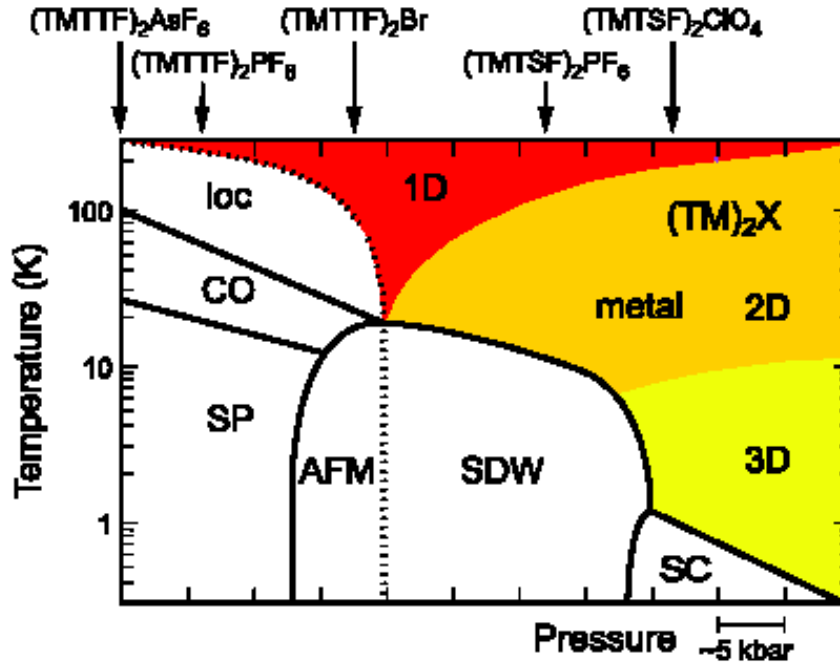


Figure 1: Schematic phase diagram of the  $(\text{TMTTF})_2\text{X}$  family. SC- superconductivity; AFM - antiferromagnet - i.e. commensurate SDW; SP - Spin-Peierls; CO- charge ordering, loc - charge localization (CO pre-translational effect); 1D,2D,3D - dimensional regimes. After Dressel, Dumm et al.

How could it happen, that such a dominant effect, which is so clear/obvious today, was missed, with so many misleading consequences? Actually there was more than enough of warnings through decades. In the prehistoric epoch<sup>3</sup>, it was the structural  $4K_F$  anomaly, for that time this discovery could also be classified as a never expected one ([37, 38, 41]; [39] for a theory,[40] for a review). Its impact upon electronic properties has been shown via the strong effect of the  $4K_F+2K_F$  lock-in [42], unfortunately this spectacular observation was washed out from memory. The coexisting  $4K_F$  and  $2K_F$  charge density waves (CDWs) with the exact trimerization were observed in NMP-TCNQ [41]; remarkably, the T dependent conductivity resembles the one of  $(\text{TMTTF})_2\text{X}$ . The sequence of transitions (spontaneous dimerization followed by the spin-Peierls (SP) tetramerization) in MEM-TCNQ [43] can be compared directly with today's cases of  $(\text{TMTTF})_2\text{PF}_6$  and  $(\text{TMTTF})_2\text{ReO}_4$ , see Sect. 5.2.

Soon after the discovery of organic superconductors, a very rich information has been accumulated on subtle structural transitions of the anion orderings (see the review [15]), but these "gifts of the magi" were not exploited as much as they deserve. As an exemption, in mid 80's the interplay of electronic and structural properties was emphasized in the earlier construction of the universal phase diagram [17, 18]; its milestones were just the cases of the intersite charge ordering in  $(\text{TMTTF})_2\text{SCN}$  and the interchain charge disproportionation in  $(\text{TMTSF})_2\text{ClO}_4$  (in contemporary language).

In retrospect of the structureless transitions, the events started to accelerate in 1997 when a theoretical work by Seo and Fukuyama [44] indicated that the AFM state may be accompanied

<sup>3</sup>A unique review connecting the science of organic metals throughout all decades is offered in [13]

by the spontaneous inequivalence of on-site occupations - the charge disproportionation. Next year, the NMR experiments by Hiraki and Kanoda [45] have allowed to register the charge disproportionation in a new compound (DI – DCNQI)<sub>2</sub>Ag, with understanding of observation of the Wigner crystallization or equivalently the condensation of the  $4K_F$  anomaly<sup>4</sup>. The SDW ordering was present indeed, but at a temperature  $T_{SDW}$  which is more than one order of magnitude lower than the charge ordering one  $T_{CO}$ . One year later, in 1999, Nad and Monceau [47], pursuing other goals of physics of sliding incommensurate SDWs, have faced the structureless transitions. Their methodic has allowed to precisely pinpoint the transition temperatures and to show that the already pronounced anomaly in microwave response [21] becomes unsustainably high in the low frequency experiments of [47]. This strong anomaly and the precise localization of its temperature have attracted the attention of the Brown group, and in 2000 they registered by the NMR the spontaneous inequivalence of sites since its very onset at  $T_{CO}$ . It took another year to finally resolve the mystery of the structureless transitions in 2001 [23]. The remarkable improvement in the experimental techniques has allowed to obtain anomalies as sharp as shown in Fig.2. This, together with the suggested theory [23, 24], left no doubt that we are dealing with a least expected phase transition to the ferroelectric state. This second order transition manifests itself in the giant anomaly of the dielectric permittivity  $\varepsilon(T)$ , Fig.2, which perfectly fits the Landau-Curie-Weiss law, Fig.7 below.

The ferroelectricity is ultimately coupled with the charge ordering, which is followed by a fast formation, or a steep increase, of the conductivity gap  $\Delta$ . There is no sign of a spin gap formation [51] or of a spin ordering down to the ten times lower scale of  $T_c$ . Hence we are dealing with a surprising ferroelectric version of the Mott-Hubbard state which usually was associated rather with magnetic orderings. The anomalous diverging polarizability is coming from the electronic system, even if ions are very important to choose and stabilize the long range 3D order. The ferroelectric transition in (TMTTF)<sub>2</sub>X is a particular, bright manifestation of a more general phenomenon of charge ordering, which now becomes recognized as a common feature of organic and some other conductors [32, 52, 33].

This rich history tells us about the necessity for reconciliation of different branches of Synthetic Metals which have been almost split for two decades<sup>5</sup>. Indeed, the major success in finding the ferroelectric anomaly was due to precise low frequency methods for the dielectric permittivity  $\varepsilon$  [53]: designed for pinned CDWs in inorganic chain conductors [54], the methods were applied also to SDWs in organic conductors [55], and finally to the structureless transitions [47]. On the theory side, the author's approach of the Combined Mott-Hubbard state [23, 56, 24, 57] has been derived from a similar experience [58, 59] in a model of conducting polymers.

## 2 Hierarchy of phases in quasi 1D organic conductors.

Low dimensional electronic systems serve as a workshop on both particular and general problems of strong correlations, degenerate collective ground states, their symmetry and topological features. The richest opportunities have been opened by the family of first quasi 1D organic superconductors: the Bechgaard - Fabre salts (TMTSF)<sub>2</sub>X, (TMTTF)<sub>2</sub>X. These compounds

---

<sup>4</sup>The charge ordering had been already found [46] in substituted perylene salts (TMP)<sub>2</sub>X (X = PF<sub>6</sub>, AsF<sub>6</sub>), which was left unattended, may be because of the accent upon effects of disorder. The charge ordering was identified via combined observations of the  $4K_F$  CDW by the X-ray and of the doubling of sites by the C<sup>13</sup> NMR.

<sup>5</sup>The conference ICSM-82 [1] was both the summit in science of Synthetic Metals and the last meeting where its all directions were present simultaneously and in mutual recognition.

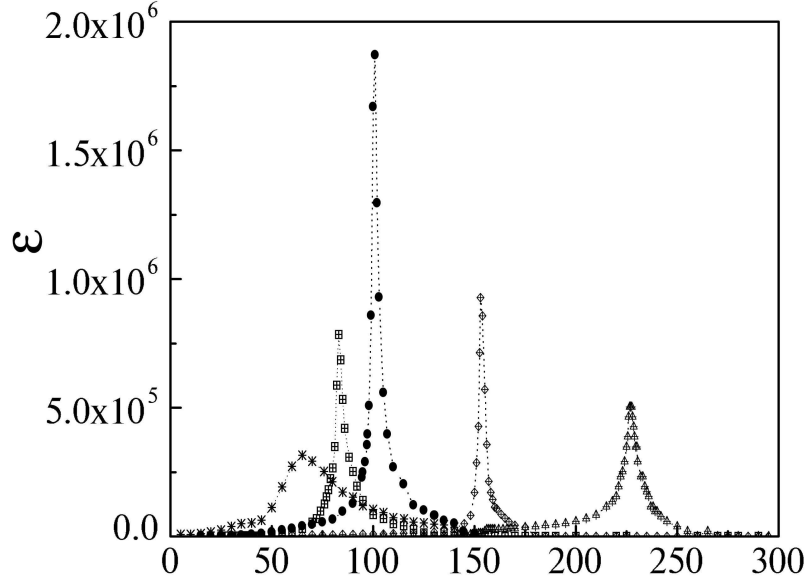


Figure 2: Linear plots of the temperature dependence of the real part of the dielectric permittivity  $\epsilon'$  at 100 kHz for  $X = \text{PF}_6$  (stars),  $\text{BF}_4$  (squares),  $\text{AsF}_6$  (circles),  $\text{SbF}_6$  (diamonds),  $\text{ReO}_4$  (triangles). After [26], see also a figure in [25]b.

demonstrate, at low temperatures  $T$ , transitions to almost all known electronic phases, see [12, 13] and Fig.1. These are: a normal metal, a regime with the Mott-Hubbard charge localization (the (para)magnetic insulator -MI in classification of [17, 18]), a spin-Peierls (i.e. a charge density wave of bonds dimerization in a framework of strong electronic repulsion), a spin density wave (SDW), an antiferromagnet (AFM) (i.e. the doubly commensurate SDW), a SDW induced by high magnetic fields (FISDW), and finally a superconductivity (SC) (of still a suggestive nature [60], see also Appendix D). Temperatures of electronic transitions  $T = T_e$  range within 1K for the SC, 10-15K for SDWs, 10-20K for the spin-Peierls phase, see Fig.1.

## 2.1 Structural transitions of the anion ordering.

There is a set of several weakly different structural types due to the anion ordering (AO) [15], which are fine arrangements of chains of singly charged counterions  $X$ . The temperatures  $T_{\text{AO}}$  of these weak structural transitions are usually about 100K. The AOs are characterized, as any superstructure, by their wave numbers  $\mathbf{q} = (q_{\parallel}, q_{\perp}) \neq 0$ , where  $q_{\parallel}$  and  $q_{\perp}$  are the components in the stack and the interstack directions. The AOs were always observed for non-centrosymmetric ions (typically tetrahedral  $X = \text{ClO}_4, \text{ReO}_4, \text{BF}_4$ , etc., except for the special case of the linear ion  $X = \text{SCN}$ ). The orientational ordering was supposed to be a leading mechanism, see [61] for a theory, with positional displacements (arrows in Fig.3) being its consequences only. But there is also a universal mechanism of the Earnshaw instability [62], inherent to all structures of classical charged particles, which can trigger independently the displacive component in materials with both centrosymmetric and non-centrosymmetric anions. (See more in the Appendix A.)

Already within the unperturbed crystal structure at  $T > T_{\text{CO}}$ , the tiny dimerization of

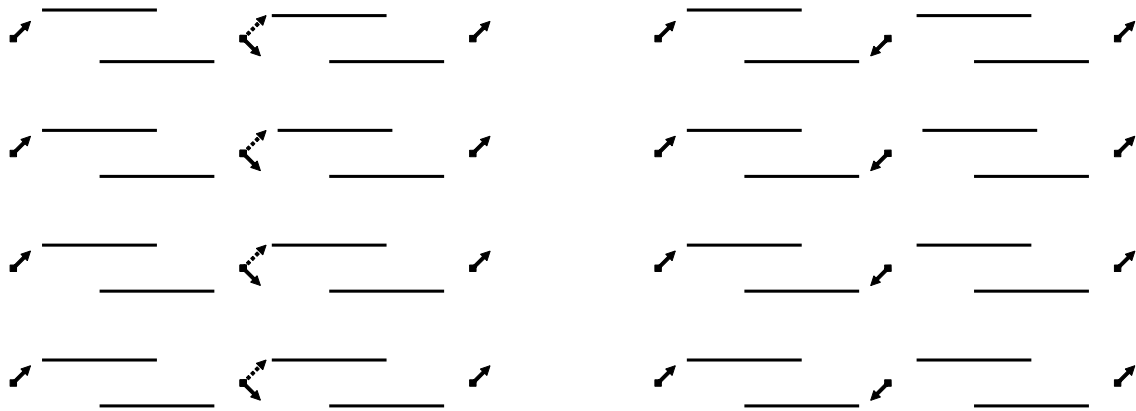


Figure 3: Structure and selected instabilities of  $(\text{TMTCF})_2\text{X}$  compounds. Horizontal bars show the molecules TMTCF, side view; the intermolecular spacings alternate. Filled squares show the anions X; arrows show displacements/orientations of ions at various AOs. Left panel:  $\mathbf{q}_2$  structure of the AFE type in  $(\text{TMTTF})_2\text{SCN}$  (all solid arrows); if the dotted arrows are chosen, then we arrive at the model for the ferroelectric ‘structureless’ phase. In both cases the molecules become nonequivalent, hence the intersite CD. Right panel:  $\mathbf{q}_3$  structure of the relaxed  $(\text{TMTSF})_2\text{ClO}_4$ . Molecular sites are kept equivalent within the chain, but chains environment alternate, hence the interchain CD. Other, tetramerized structures are shown in [15].

bonds by anions X in  $(\text{TMTCF})_2\text{X}$  provokes the dielectrization [63, 64, 18]. Regular alternation of ions, positioned against every second intermolecular spacing, dimerizes the intermolecular distances. It doubles the on-stack unit cell, hence changes the mean electronic occupation from  $1/2$  per molecule to 1 per dimer. The bond alternation gives rise [63] to the relatively small Umklapp scattering  $U_b$ , which opens (according to Dzyaloshinskii and Larkin [65], Luther and Emery [66, 67], see Sects. 4,8) the route to the Mott-Hubbard insulator. (See [56] and [68] for a history introduction and Appendix D for some quotations).

## 2.2 Charge ordering transitions.

At similar or even higher range,  $T = T_{\text{CO}} \approx 100 \div 200\text{K}$ , also other unidentified transitions were observed sometimes in the TMTTF subfamily. Their signatures were seen in conductivity [19], microwave permittivity [21], in thermopower [20]. But there was no trace of any lattice effects, hence the title ‘structureless’ transitions was assigned. Recently their mysterious nature has been elucidated by discoveries of the huge anomaly in the dielectric permittivity  $\varepsilon$  at  $T_{\text{CO}}$  [23, 25] and of the charge disproportionation seen by the NMR [27] at  $T < T_{\text{CO}}$ . It is still an experimental challenge to refine the structure; a scheme for its reconstruction is outlined in this section.

The ferroelectric anomaly signifies that the term ‘structureless’ is not quite correct: this is not an isomorphic modification. While the Bravais lattice is based on the same unit cell indeed, the full space symmetry is changed by losing the inversion center, which is the necessary condition for the ferroelectric state.

The NMR experiments [27] have clearly detected the appearance at the  $T_{\text{CO}}$  of the site nonequivalence as a sign of the CO/CD. Recently the charge disproportionation was also confirmed by means of the molecular spectroscopy [69], see Fig. 17 below. While bonds are usually

dimerised already within the basic structure, see Fig. 3, the molecules stay equivalent above  $T_{CO}$ , the latter symmetry being lifted by the charge ordering transition. At presence of the inequivalence of bonds, the additional inequivalence of sites lifts the inversion symmetry, hence the allowance for the chain's polarization leading to the ferroelectricity.

The confidence for this identification comes from a good fortune, that the 3D pattern of the charge ordering appears in two, AFE and FE, forms. Both types AFE and FE are the same paramagnetic insulators (the MI phase of [17, 18]), which is shown by comparison of electric and magnetic measurements. The NMR brought the same observation [27] both for the structureless transitions and for the particular AFE phase in  $(TMTTF)_2SCN$ ; also the permittivities at high frequencies and temperatures are very similar. The structure of the  $(TMTTF)_2SCN$  has been already known as a very rare type of  $\vec{q}_2 = (0, 1/2, 1/2)$ . The site inequivalence was already identified by the structural studies, see [15] and Fig. 3. The structure was completely refined; the anions displacements are unilateral for each column while undulating among them.

So, what is the difference between the  $\vec{q}_2$  case and the 'structureless' transitions? The  $\vec{q}_2$  structure showed already the common polarization along a single stack,  $q_{\parallel} = 0$ , but alternating in perpendicular directions,  $\vec{q}_{\perp} \neq 0$ , Fig. 3; it gives, as we can interpret today, the AFE ordering. For the 'structureless' transition all displacements must be identical  $\vec{q} = 0$  among the chains/stacks, thus leading fortunately to the ferroelectric state. We arrive at the quite sound conjecture that the ferroelectric 'structureless' state corresponds to the scheme of Fig. 3 where we should choose the dotted arrows instead of solid ones. Without the advantage of having the structural information [15] on the  $(TMTTF)_2SCN$ , our understanding of the nature of the ferroelectric compounds would be more speculative. This case can be viewed as a corner-stone, or Rosetta stone, in a sense that it belongs to two classes of anion ordering and charge ordering systems and transfers a complementary information.

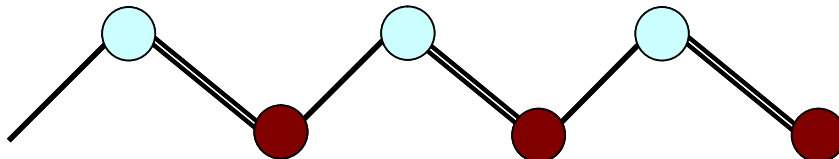


Figure 4: The scheme of a conjugated polymer of the  $(AB)_x$  type, realized recently as the modified polyacetylene [75]. Dark and light circles correspond to chemically inequivalent monomers (actually the carbon atoms with different ligands). Single and double connections show the expected spontaneous dimerization of bonds. Curiously, this model takes just the form of the hypothetical design by W. Little for a polymeric superconductor (D. Jerome, introduction to ISCOM-03 [3]), which suggestion gave birth to the whole science of Synthetic Metals.

In any case, FE or AFE, the polar displacement gives rise to the joint effect of the built-in and the spontaneous contributions to the dimerization, due to alternations of both bonds and sites<sup>6</sup>. None of these two types of dimerization changes the unit cell of the zigzag stack which basically contains two molecules, hence  $q_{\parallel} = 0$  for the charge ordering wave vector. But their sequence lifts the mirror (glide plane) and then the inversion symmetries which must lead

---

<sup>6</sup>Both contributions can be of the built-in type in the particular case of the  $(TMTSF)_{0.5}(TMTTF)_{0.5}$  mixture [70], where the alternation of S/T-containing molecules provides the site dimerization. Oppositely, both coexisting dimerizations may appear spontaneously, but these two independent symmetry breakings require for two successive second order phase transitions or for the first order one. The later option may be relevant to observations [31, 34].



to the on-stack electric polarization. This interference resembles the orthogonal mixing in the "combined Peierls state" [58] in conjugated polymers of the  $(AB)_x$  type, Fig. 4. Here also the bond dimerization is the  $q_{\parallel} = 0$  transition, just because of the backbone zigzag structure: what looks for electrons as a period doubling, is structurally the lifting of the glide plane symmetry.

### 2.3 Overlapping and coexistence of phases.

The 'structureless' displacive instability and the usual 'orientational' AOs can be independent. This is supported by finding of a sequence of the ferroelectric and the anion ordering transitions in  $(\text{TMTTF})_2\text{ReO}_4$  [25]. We will show in Sect. 5.2 that this true present from the Nature gives an access to compound solitons, as to intriguing events of the spin-charge reconfinement. At the same time, the case of  $(\text{TMTTF})_2\text{SCN}$ , where  $q_{\parallel} = 0$  while  $q_{\perp} \neq 0$ , presents the corner-stone belonging to both types of AOs and charge ordering transitions.

Notice finally that the  $q_{\parallel} = 0$  structure is not ultimately the on-chain charge ordering. The so-called  $\vec{q}_3 = (0, 1/2, 0)$  type of the anion ordering [15], observed in the relaxed phase of the  $(\text{TMTSF})_2\text{ClO}_4$ , shows the interchain redistribution of charges. This is a kind of the "incommensurability transition" (with an unusually reversed order in comparison with the conventional lock-in to the commensurable state) which may be considered [17, 18] as a prerequisite of the superconductivity.

### 2.4 Electronic mechanism of the charge ordering.

To get an idea of the driving force behind the hidden 'structureless' transition we shall follow the example of the "combined Peierls state" [71, 72] developed for polymers like the modified polyacetylene. It describes a joint effect of built-in and spontaneous contributions to the dimerization, hence to the electronic gap. Since this concept was formulated [73], it has been widely used in studies of conducting polymers gaining a clear experimental support in diverse observations, especially in optics and ESR, see [74]. Particularly relevant is the experimentally recent [75] case of the "orthogonal mixing" relevant to polymers of the  $(AB)_x$  type, Fig. 4. Here the built-in gap  $\Delta_s$  comes from the site dimerization due to the  $AB$  alternation, while the spontaneous contribution to the total gap  $\Delta$  comes from the dimerization of bonds  $\Delta_b$ , like in the generic Peierls effect. Importantly, the two gaps add in quadrature:  $\Delta = \sqrt{\Delta_{in}^2 + \Delta_{ex}^2}$  - the amplitudes of electron's scattering, Fig. 11 - right, are shifted by  $\pi/2$ .

For the present case of the charge ordering, the Peierls effect is substituted by the Mott-Hubbard one. Also the built-in and the spontaneous effects are interchanged: the built-in one comes from inequivalence of bonds while the spontaneous one comes from non equivalence of sites. The charge gap  $\Delta = \Delta(U)$  appears as a consequence of both contributions to the Umklapp scattering, and it is a function of the total amplitude  $U = \sqrt{U_s^2 + U_b^2}$ . (But the observable gap  $\Delta(U)$  is not additive in quadratures any more.)

The electronic energy  $F_e$  depends only on the charge gap  $\Delta$ , which is a function of only the total  $U = \sqrt{U_s^2 + U_b^2}$ . The energy of lattice distortions  $F_l$  depends only on the spontaneous site component  $U_s$ :  $F_l = (K/2)U_s^2$ , where  $K$  is an elastic constant. Thus the total energy can be written in terms of the total  $U$ :

$$F(U) = F_e(U) + 1/2KU^2 - 1/2KU_b^2, \quad U \geq U_b$$

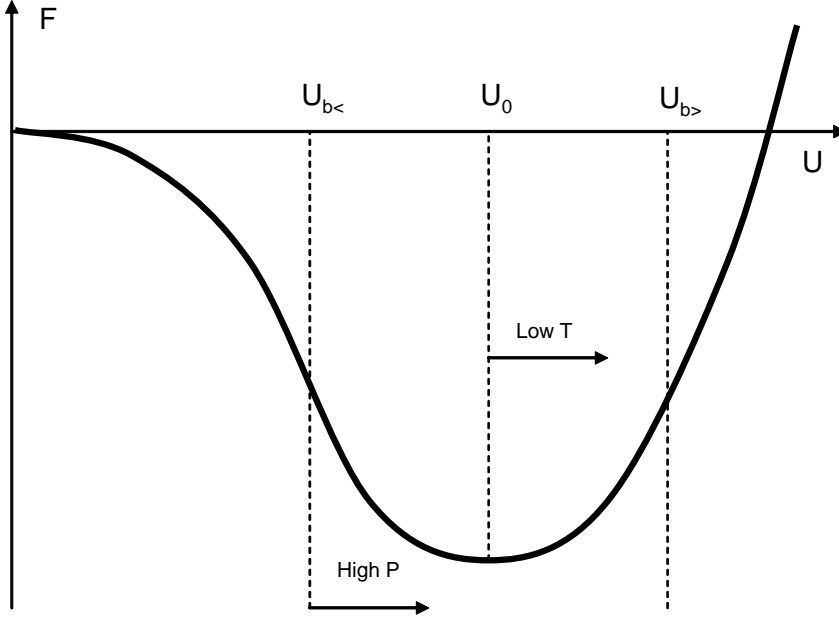


Figure 5: Ground state energy  $F(U)$  as a function of the total magnitude  $U = \sqrt{U_s^2 + U_b^2}$  of the commensurability (Umklapp) potential. Its minimum at  $U_0$  is reachable if  $U_b < U_0$  corresponding to the position  $U_{b<}$ ; then the spontaneous  $U_s$  is created to augment  $U_b$  to  $U_0$ . It does not happen, if  $U_b > U_0$  corresponding to the position  $U_{b>}$ , then there is no transition. The arrows show that these two regimes can interchange by either changing of  $U_0$  by temperature or of  $U_b$  by pressure.

The ground state is determined by its minimum over  $U$ , but unusually at the constraint  $U \geq U_b$ . We can encounter three possibilities for the energy function  $F(U)$ , Fig.5.

- It has no minimum except  $U = 0$ : no charge ordering at any condition;
- It has a minimum at some value  $U = U_0 < U_b$ : charge ordering is possible but not reached yet;
- It has a minimum at some value  $U = U_0 > U_b$ , which now determines the ground state. Since the value  $U_0$  increases with decreasing temperature, there will be a phase transition at  $U_0(T) = U_b$  provided that  $U_0(0) > U_b$ .

The phase transition in the regime (c) can be reversed if  $U_b$  is made to increase passing above  $U_0$ , then the charge ordering disappears. This is what seems to happen typically in experiments under pressure [104, 105].

How does this minimum at  $U_0$  appear actually? In principle, the electron energy  $F_e(U) < 0$  is always gained by opening the gap  $\Delta$  which reduces the zero point fluctuations. But to overcome the energy loss  $\sim U_s^2$  from lattice deformations and charge disproportionation, we need  $F_e(U) \sim -U^{2-\zeta}$  with  $\zeta \geq 0$ . For conventional  $2K_F$  CDWs it is always the case with  $F_e(U) \sim -U^2 \ln E_F/U$  corresponding to the limit  $\zeta \rightarrow 0$ . For our case of the  $4K_F$  modulations the condition is reached only at large enough interactions [39] with the marginal case  $\zeta = 0$  corresponding to the so-called Luther-Emery line [66, 67], see more in Sect.4. We can view it also as a general criterium of the  $4K_F$  instability [39].

## 2.5 Electric polarization and Ferroelectricity.

In principle, there are three contributions to the electric polarizability:

1. *Intergap electronic polarizability* is regular at  $T_{\text{CO}}$ :  $\varepsilon_{\Delta} \sim \omega_p^2/\Delta^2$ , where  $\omega_p$  is the plasma frequency. At the transition, where  $\Delta(T \approx T_{\text{CO}})$  is still well below its low  $T$  value  $\Delta(0)$ ,  $\varepsilon_{\Delta}$  can be as large as  $\sim 10^3$  which corresponds indeed to the background upon which the anomaly at  $T_{\text{CO}}$  is developed. The value of the gap well corresponds to the lower  $\varepsilon_{\Delta} \approx 100$  as it was estimated already in [21].
2. *Ion displacements* could already lead to the macroscopic polarization, like in usual ferroelectrics, but taken alone they cannot explain the observed giant magnitude of the effect. Taking the typical parameters [15] of AOs (recall the SCN case as the corner-stone), the ionic displacive contribution may be estimated (see Appendix B.1) as  $\varepsilon_i \sim 10^4 T_{\text{CO}}/|T - T_{\text{CO}}|$ , which is by  $10^{-3}$  below a typical experimental value  $\varepsilon \approx 2.5 \times 10^4 T_{\text{CO}}/(T - T_{\text{CO}})$  [23].
3. *Collective electronic contribution* can be estimated roughly [23], see Appendix B.1, as a product of the above two  $\varepsilon_{el} \sim \varepsilon_i \varepsilon_{\Delta}$ , which provides both the correct  $T$  dependence and the right order of magnitude of the effect. The anomalous diverging polarizability is coming from the electron subsystem, even if the instability is triggered by the ions, whose role is to stabilize the long range 3D ferroelectric order, and to discriminate between FE, AFE, or more complex patterns [31], see more in the Appendix B.2.

## 3 Electronic properties.

Here we shall give a short summary of experimental results on electronic properties of  $(\text{TMTTF})_2\text{X}$  compounds <sup>7</sup>.

### 3.1 Permittivity.

Typical plots of the temperature dependence of the dielectric permittivity  $\varepsilon^8$  at Figs.2,6, demonstrate very sharp (even in the log scale of Fig. 6!) ferroelectric peaks. Most of cases show the purely mono-domain "initial" ferroelectric permittivity, ideally fitting the Curie law  $\varepsilon \sim |T - T_{\text{CO}}|^{-1}$ , Fig. 7 - even with the right ratio = 2 of the Landau theory for inclinations at  $T \gtrsim T_{\text{CO}}$  [23] <sup>9</sup>. In general, we observe the frequency dependent depolarization of the mono domain ferroelectricity, instead of the more usual long time hysteresis of the re-polarization. Still abundant normal carriers screen the ferroelectric polarization at the surface, which eliminates the need for the domain structure. Low-temperature studies are necessary to find the remnant polarization. Radiational damage or other disorder will also help to pin the domain walls and freeze the polarization, which should give rise to the conventional hysteresis curve.

The AFE case of  $\text{X} = \text{SCN}$  in Fig. 6 shows a smooth maximum of  $\varepsilon$ , rather than a divergent peak, as it should be. Nevertheless, the high  $T$  slopes of all curves for  $\varepsilon(T)$  look very similar. It tells us that the ferroelectric state is gradually developing already within the high  $T > T_{\text{CO}}$  1D regime, before the 3D interactions discriminate between the in-phase FE and the out-of-phase AFE orderings. Recall that, contrary to these low frequencies, in the microwave range

<sup>7</sup>Experimental plots of this chapter are the results by Monceau, Nad, et al, see [25, 26] for a broad collection.

<sup>8</sup>We imply everywhere, unless specified, the real part of  $\varepsilon$ :  $\Re\varepsilon = \varepsilon'$

<sup>9</sup>A relatively rounded anomaly in the  $\text{PF}_6$  case of Fig. 7 correlates with its stronger frequency dispersion, Fig. 8: it can be a pinning of ferroelectric domain walls, in other words a hidden hysteresis. For an extended information on frequency dispersion, see [48, 50] and the review [26].

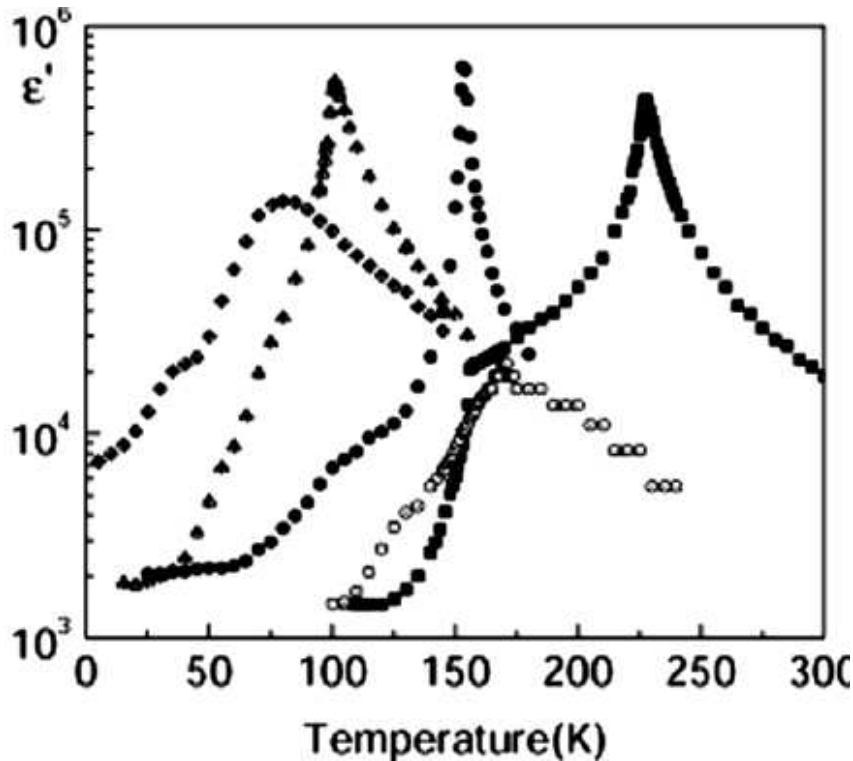


Figure 6:  $\log \varepsilon'$  vs  $T$  at  $f=1\text{MHz}$  for FE cases  $X = \text{PF}_6$  ( $\diamond$ ),  $\text{AsF}_6$  ( $\triangle$ ),  $\text{SbF}_6$  ( $\bullet$ ),  $\text{ReO}_4$  ( $\blacksquare$ ) and for the AFE  $X = \text{SCN}$  ( $\odot$ ). After [25].

the  $X=\text{SCN}$  compound showed [21] the strongest response with respect to ferroelectric cases; hence the purely 1D regime of the ferroelectricity was recovered. This may also be the key to the AFE/FE choice. Indeed, for highly polarizable units containing the already polar ion SCN, the dominating Coulomb forces will always lead to an AFE structure.

The  $X = \text{ReO}_4$  case shows at 150K a subsequent first order anion ordering transition of tetramerization. Here  $\varepsilon$  drops down (Fig. 6, see also [25, 26] for details) which might be caused (via the factor  $\omega_p^2/\Delta^2$ ) by the increase of the gap  $\Delta$  as it is seen at the conductivity plot in Fig. 10. The case of  $X = \text{PF}_6$  shows the spin-Peierls transition at  $T=19\text{K}$ . While being symmetrically equivalent to the anion ordering in  $X = \text{ReO}_4$  case, it is of the second order, so that in  $\varepsilon(T)$  it shows up only as a shoulder.

### 3.2 Conductivity.

Fig. 9 gives several examples of the conductivity  $G(T)$  within the high  $T$  region around  $T_p$ . Fig. 10 shows, for selected examples, the conductivity  $G(T)$  within a broad range of temperatures (see more cases in [25, 26]). Typical plots correlate with old data [21]<sup>10</sup>, but with more insight available today:

1) Clear examples for conduction by charged spinless particles - holons = solitons: there are no gaps in spin susceptibility  $\chi \approx \text{const}$  [51];

<sup>10</sup>In reviewed experiments by Nad, Monceau et al, the conductivity was extracted via  $\Im \varepsilon$ , within the same experiment as measuring the  $\text{Re} \varepsilon$ .

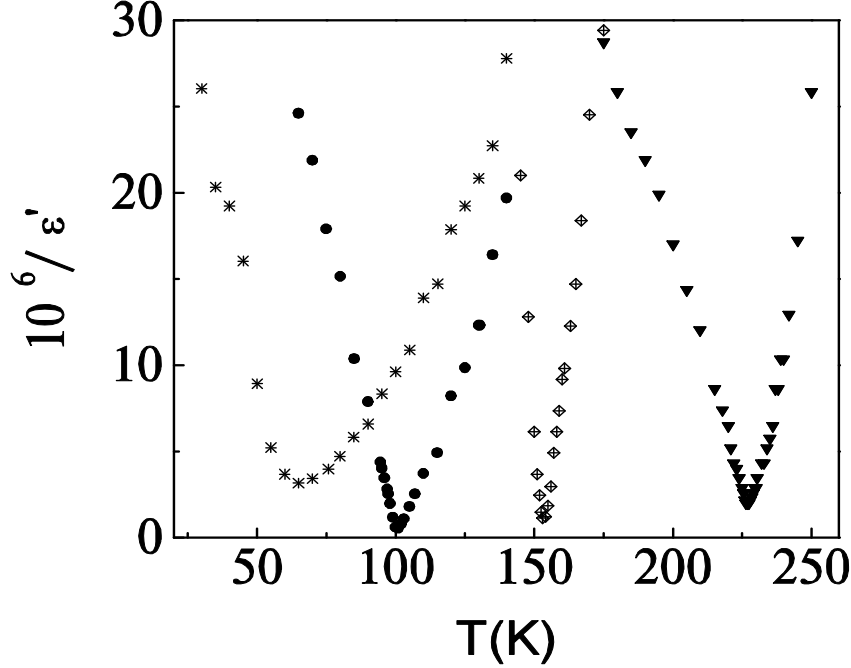


Figure 7: Temperature dependence of the inverse of the real part of the dielectric permittivity  $\epsilon'$  of  $(\text{TMTTF})_2\text{X}$  with  $\text{X} = \text{PF}_6, \text{AsF}_6, \text{SbF}_6, \text{ReO}_4$  (in the order from left to the right) at the frequency of  $100\text{Hz}$ . After [23, 25].

2) There is no qualitative difference in  $G(T)$  (as well as in NMR ! [27]) between FE cases and the AFE one of the SCN: only the on-chain charge ordering is important, not the type of the interchain pattern!

3) Coexistence of both types of transitions, CO and AO, in  $(\text{TMTSF})_2\text{ReO}_4$ ; the subsequent anion ordering increases the conduction gap and opens the spin gap [77].

4) Gap contribution of the spontaneous site dimerization develops very fast, and soon it dominates over the bond dimerization gap. The last may not be seen at all – recall that the ferroelectric anomaly extends by at least 30K above  $T_{\text{CO}}$ , Fig. 7, signifying the pre-translational CO, which is able to workout a pseudogap.

At  $T < T_{\text{CO}}$  the charge ordering adds more to the charge gap  $\Delta$ , which is formed now by joint effects of alternations of bonds and sites. The conductivity  $G(T)$  plots in Fig. 9 show this change by kinks at  $T = T_{\text{CO}}$ , turning down to higher activation energies at low  $T$ . The steepness of  $G$  just below  $T_{\text{CO}}$  reflects the growth of the charge ordering contribution to the gap, which is expected to be  $\delta\Delta(T) \sim \sqrt{T_{\text{CO}} - T}$ , see section 4; it must correlate with  $\epsilon^{-1} \sim (T_{\text{CO}} - T)$ . Indeed, what may look as the enhanced gap (the tangent for the Arrhenius plot) near  $T_{\text{CO}}$ , actually can be its  $T$  dependence expected as  $\Delta(T) = \sqrt{\Delta_b^2 + C\Delta_s(0)(1 - T/T_{\text{CO}})}$ ,  $C \sim 1$ . The differential plotting of  $\Delta(T) = -d \log G / d(1/T)$  would be helpful.

So marginal effect of the built-in bond dimerization opens the route to compounds with equivalent bonds [45, 22, 30, 78].

$(\text{DMtTTF})_2\text{ClO}_4$ : Here, the ordered state has been already identified [31] as a complex (incommensurate in the transverse direction) AFE structure, which develops following a fasci-

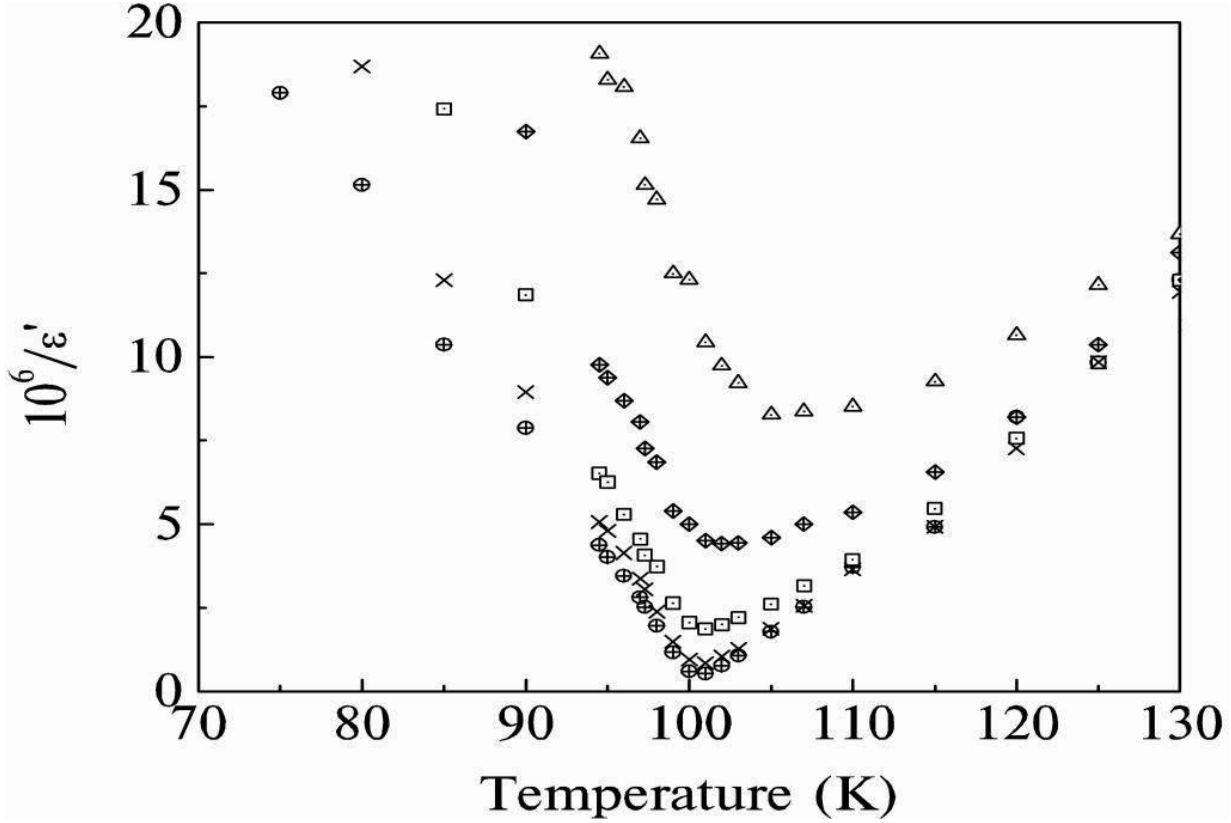


Figure 8: Plots of  $10^6/\epsilon'(T)$  of  $(\text{TMTTF})_2\text{AsF}_6$  at 10000, 3000, 1000, 300, 100 KHz. Nad, Monceau et al, unpublished.

nating pseudo-first order phase transition at  $T=150\text{K}$ . This material shows [22] the characteristic resistivity rise below quite typical  $T_\rho \approx 120 - 150\text{K}$ , which does not affect, as expected, the susceptibility  $\chi$  until the low  $T_{SDW} \approx 10\text{K}$  AFM ordering. The charge ordered phase is waiting to be tested for the NMR splitting and for the  $\epsilon$  anomaly, or at least for traditional signatures of structureless transitions like the thermopower.

(EDT – TTF – CONMe<sub>2</sub>)<sub>2</sub>X: A similar situation is expected in this new material [22, 30, 78], which is also the Mott insulator with the conductivity gap  $\approx 1350\text{K}$ . Unfortunately, there is a lack of information for this compound; vaguely it was declared [78] as a clear case of 4-fold commensurability effects, following the "no CO/CD" scenario for  $(\text{TMTCF})_2\text{X}$  family, see Sec. 8.2.

(DI – DCNQI)<sub>2</sub>Ag: The nondimerized compound, where the observation of the charge ordering [45] has started the modern trend. Here also the activation energy value  $\approx 490\text{K}$  is well above the  $T_{\text{CO}} \approx 220\text{K}$ .

Now we can close the circle to return to the  $(\text{TMTTF})_2\text{X}$  series and to guess that the observed conductivity downturn at  $T_\rho > T_{\text{CO}}$  may be mostly due to the fluctuational pseudogap coming from the charge ordering proximity. There may be only a minor contribution from the bond dimerization specific to  $(\text{TMTTF})_2\text{X}$ .

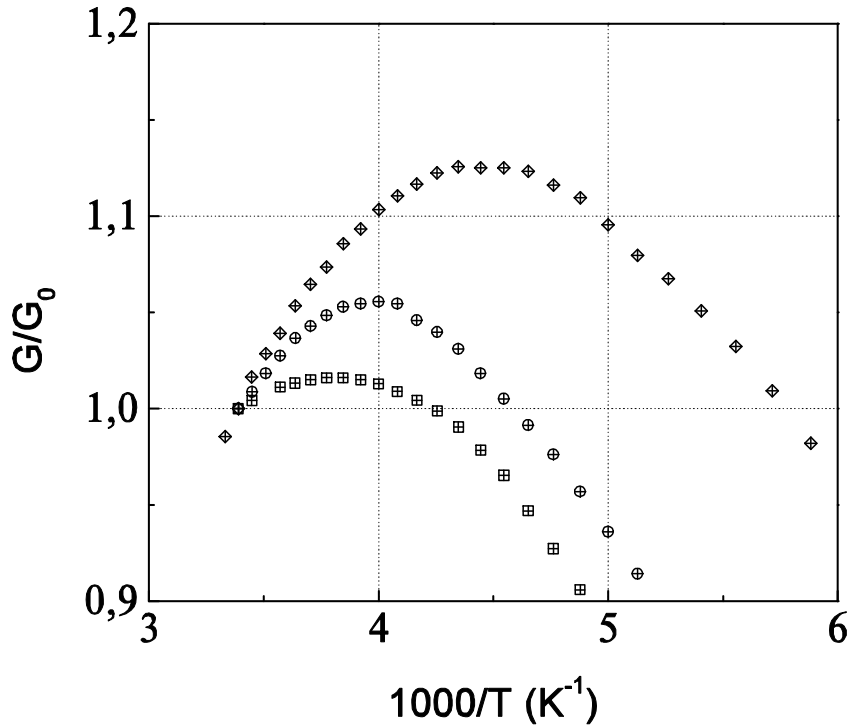


Figure 9: Plots for the normalized conductivities  $G/G_0$  ( $G_0$  is the RT value) in the  $T \approx T_\rho$  region. X = SbF<sub>6</sub> (squares), AsF<sub>6</sub> (circles), PF<sub>6</sub> (diamonds). The plots  $G(T)$  show maxima at  $T = T_\rho > T_{CO}$ . After [25, 26].

## 4 Ferroelectric Mott-Hubbard ground state.

### 4.1 Choosing the theory approach.

The earliest theoretical prediction [44] applies literally to a situation expected in 3D, or at most 2D systems, where the charge ordering is set up simultaneously and in ultimate conjunction with the AFM/SDW order. In (TMTTF)<sub>2</sub>X type cases, the pronouncedly 1D electronic regime brings its particular character, as well as it allows for a specifically efficient treatment [23], which also happens to be particularly well suited to describe the ferroelectric transition.

We are using the bosonization procedure, see reviews [67, 79, 80], which is most adequate to describe low energy excitations and collective processes. It takes into account automatically the separation of spins and charges, which is a common feature of our systems. All information about basic interactions, whatever they are (on-site, neighboring sites, long range Coulomb, lattice contribution, see Sect. 8.1) is concentrated in a single parameter ( $\gamma = K_\rho$  - in modern notations). This approach allows to efficiently use the symmetry arguments and classification. It allows to naturally interpret the solitonic spinless nature of elementary excitation - the thermally activated charge carriers. Most importantly for our goals, this approach provides a direct access to the dielectric permittivity. The procedure easily covers also the secondary anion ordering or spin-Peierls transitions at lower  $T$ . A rigorous way to describe a correlated 1D electronic system, bosonization also provides a physically transparent phenomenological interpretation in terms of fluctuating  $4K_F$  density wave, i.e. a local Wigner crystal, subject to a weak commensurability

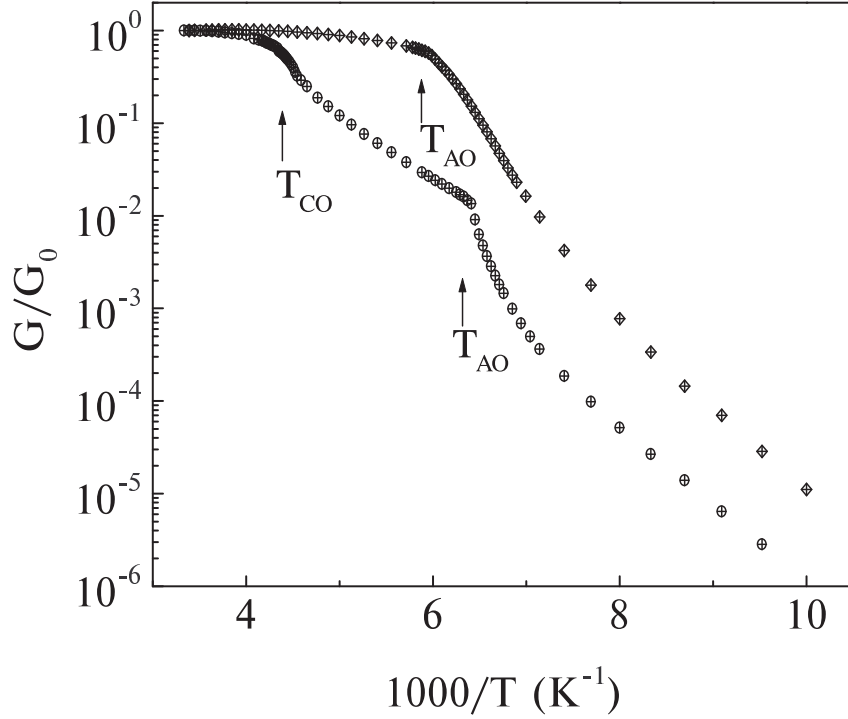


Figure 10: Ahrenius plots for normalized conductivities  $G/G_0$  in a wide  $T$  region.  $X = \text{ReO}_4$  ( $\circ$ ),  $X = \text{SCN}$  ( $\diamond$ ). After [76, 24].

potential. See more arguments in [18], and some quotations in Appendix D.

Among other approaches, recall also the traditional line of RG theories in recent quasi 1D versions [81, 82]. The today's results do not pass the major test for the charge ordering (at least it was merely overlooked), hence they cannot be applied to  $(\text{TMTTF})_2\text{X}$  type cases, even if a work was deducted to this purpose [81].

Recall also numerical studies like exact diagonalization of small clusters with short range interactions or quantum chemistry methods [83, 84]. Usually they pass the test for the charge ordering, but experience difficulties to obtain its ferroelectric type as the most favorable one. Even in case of a success for the ground state, the access to polarization and to elementary excitations will not be sufficient, or even possible, particularly for more sophisticated cases of combined symmetry breakings, Sect. 5.2.

## 4.2 Ground state and symmetry breaking.

We introduce the charge phase  $\varphi$  as for  $2K_F$  CDW or SDW modulations  $\sim \cos(\varphi + (x - a/2)\pi/2a)$  - the origin is taken at the inversion center in-between the two molecules. Here  $a$  is the intermolecular distance; recall that  $\pi/4a = K_F$  is the Fermi number in the metallic praphase. Later on we shall need also the spin counting phase  $\theta$ :  $\varphi$  and  $\theta$  together define the CDW order parameters completely as  $\mathcal{O}_{CDW} \sim \exp(i\varphi) \cos \theta$ . Gradients of these phases  $\varphi'/\pi$  and  $\theta'/\pi$  give local concentrations of the charge and the spin. The energy density (potential and kinetic) of



charge polarizations is

$$\frac{1}{4\pi\gamma} \{(\partial_x \varphi)^2 v_\rho + (\partial_t \varphi)^2 / v_\rho\} \quad (1)$$

Here  $v_\rho \sim v_F$  is the charge sound velocity and  $\gamma$  is the main control parameter, which depends on all interactions; its origin is discussed in Sect. 8.1. ( $\gamma$  is the same as  $\gamma_\rho$  of [17, 18] or  $K_\rho$  of our days.)

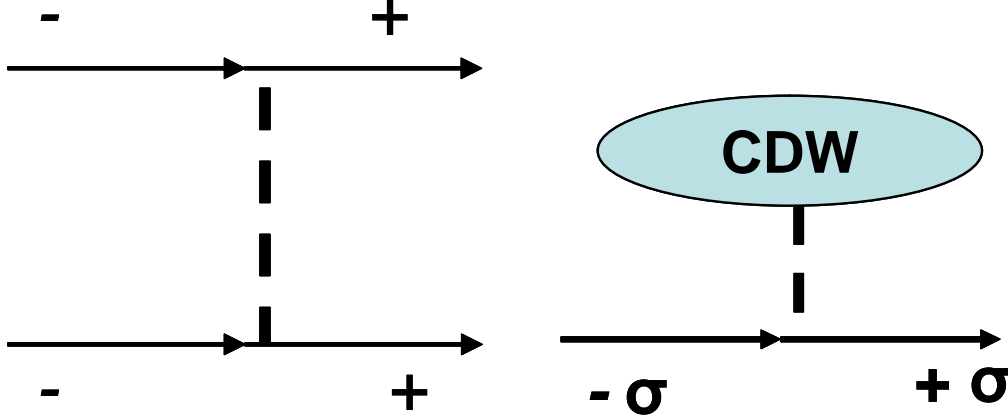


Figure 11: Umklapp processes. Left: an electron pair is scattered from  $-K_F$  to  $+K_F$ ; the quasi-momentum deficiency  $4K_F$  is absorbed by the periodicity of the dimerised lattice. Right: at presence of the tetramerization providing the  $2K_f$  CDW background, a single electron is scattered from  $-K_F$  to  $+K_F$  (conserving the spin  $\sigma$ ); the deficiency  $2K_F$  is absorbed by the CDW order corresponding to the tetramerization.

In addition to (1), there is also the commensurability energy  $H_U$  coming from the Umklapp scattering of electrons, Fig. 11a-left. For our particular goals it is important to notice several interfering sources for the weak two fold commensurability, i.e. two contributions to the Umklapp interaction. Their forms can be derived from the symmetry alone [23], as we shall sketch now.

Consider the non dimerized system with  $1/2$  electrons per site. It possesses translational and inversion symmetries  $x \rightarrow x + 1$  and  $x \rightarrow -x$  which corresponds to phase transformations  $\varphi \rightarrow \varphi + \pi/2$  and  $\varphi \rightarrow -\varphi$ . The lowest order invariant contribution to the Hamiltonian is  $H_4 \sim U_4 \cos 4\varphi$ . This is the 4-fold commensurability energy which is usually very small, recall the conventional CDWs. The reason is not only a smallness of  $U_4$  which is coming from Umklapp interaction of 8 particles, half of them staying high away from the Fermi energy. In addition, it is renormalized as  $\sim \exp[-8 \langle \varphi^2 \rangle]$ , that is it becomes small, being a product of two large numbers in the negative exponent, see more in Sect. 8.2.

Consider next the site dimerization which modulates alternatively the onsite energies. The preserved symmetries are  $x \rightarrow x + 2$  and  $x \rightarrow 1 - x$  (reflection with respect to the molecular cite center). Hence the invariance is required with respect to  $\varphi \rightarrow \varphi + \pi$  and  $\varphi \rightarrow \pi/2 - \varphi$  and we arrive at  $H_U^s = -U_s \sin 2\varphi$ .

Consider finally the bond dimerization. The symmetry  $x \rightarrow x + 1$  is broken while the symmetries  $x \rightarrow x + 2$  and  $x \rightarrow -x$  are preserved. The Hamiltonian must be invariant under the corresponding transformations of  $\varphi$ :  $\varphi \rightarrow \varphi + \pi$  and  $\varphi \rightarrow -\varphi$  and we arrive at  $H_U^b = -U_b \cos 2\varphi$ .

At presence of both types of dimerization, the nonlinear Hamiltonian, to be added to (1), becomes

$$\begin{aligned} H_U &= -U_b \cos 2\varphi - U_s \sin 2\varphi = -U \cos(2\varphi - 2\alpha) ; \\ U &= (U_b^2 + U_s^2)^{1/2}, \tan 2\alpha = U_s/U_b \end{aligned} \quad (2)$$

The  $4k_F$  charge modulation will be

$$\rho_{4K_F} \sim \psi_-^2 \psi_+^{\dagger 2} + HC \sim \cos(\pi x/a + 2\alpha) = (-1)^{x/a} \cos(2\alpha)$$

where  $\psi_{\pm}$  are one-electron operators near the points  $\pm K_F$ . The  $2K_F$  bond and site CDWs are proportional to

$$\rho_{2K_F}^{b,s} \sim \{\psi_- \psi_+^{\dagger} \mp h.c.\} \sim \cos \theta \{\cos, \sin\}(\pi x/2a + \alpha)$$

Their mean values are zero, because of the spin factor which vanishes in average  $\langle \cos \theta \rangle = 0$  until the spin gap is established below the spin-Peierls temperature, see Sect. 5.2.

The  $U_s$  comes from the electronic charge ordering and ionic displacements coupled by long range 3D Coulomb and structural interaction, which are well described by the mean field approach. But the electronic degrees of freedom must be treated exactly at a given  $U_s$ . The renormalization, due to quantum fluctuations of phases, leaves the angle  $\alpha$  invariant, but it reduces  $U$  in (3) down to  $U^* \sim \Delta^2/\hbar v_F$  ( $U^* \neq 0$  only at  $\gamma < 1$ ); it determines the gap  $\Delta \sim U^{1/(2-2\gamma)}$ . (In scaling relations, we imply units  $E_F$  for  $\Delta$  and  $E_F/a$  for  $U$ .) The spontaneous charge ordering  $U_s \neq 0$  requires that  $\gamma < 1/2$ , far enough from  $\gamma = 1$  for noninteracting electrons. The magnitude  $|U_s|$  is determined by competition between the electronic gain of energy and its loss  $\sim U_s^2$  from the lattice deformation and charge redistribution (recall Sect. 2.4 and Appendix B.2). 3D ordering of signs  $U_s = \pm |U_s|$  discriminates the FE and AFE states.

A conceptual conclusion is that the Mott-Hubbard state can be energetically favorable, then the system will mobilize an available auxiliary parameter to reach it. In our case, this parameter is the site disproportionation, which very fortunately is registered as the ferroelectricity.

## 5 Elementary excitations.

### 5.1 Solitons.

#### 5.1.1 Solitons seen in most common cases.

For a given  $U_s$ , the ground state is doubly degenerate between  $\varphi = \alpha$  and  $\varphi = \alpha \pm \pi$ , which allows for phase  $\pm\pi$  solitons [85] with the energy  $E_{\pi} = \Delta$ ; they are the charge  $\pm e$  spinless particles - the (anti)holons. Fig. 12 illustrates the origins of the potential  $U_s \sin(2\varphi)$  by showing the sequence of zeros and extrema  $\pm 1$  of the electron wave function  $\Psi$  taken at  $E_F$ . The upper row corresponds to one of two correct ground states, energy minima at  $\varphi = 0, \pi$ . The degeneracy " $\Psi = \pm 1$  at good sites" gives rise to  $\pi$ -solitons as kinks between these two signs of the wave function, Fig. 13 - left.

The  $\pi$  solitons always determine the conductivity at  $T < T_{\rho}$ . Thus in  $(\text{TMTCF})_2\text{X}$  they are observed in conductivity at both  $T \gtrsim T_{\text{CO}}$ ; in compounds without the built-in dimerization - at  $T < T_{\text{CO}}$ . An expected characteristic feature of solitonic conductivity is its strong reduction and enhanced activation energy for the conductivity in the interchain direction as it has been observed

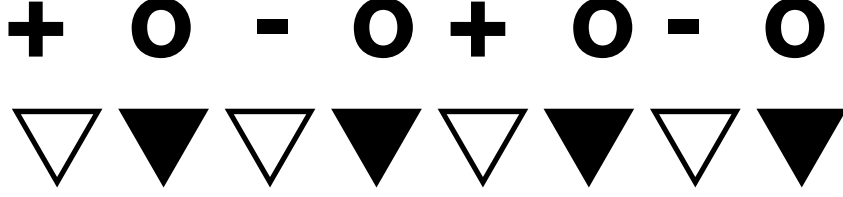


Figure 12: Degeneracy scheme for electrons on a lattice with the site dimerization. Lower row: white/black triangles show the good/bad sites. Upper row: signs  $\pm$  and zeros of the electronic wave function at  $E_F$ . Shown configuration:  $\varphi = 0$  or  $\pi$ :  $\Psi = \pm 1$  or  $\Psi = \mp 1$  at good sites and  $\Psi = 0$  at bad sites.

in  $(\text{TMTTF})_2\text{X}$  [86]. Dynamics of solitons have been accessed in recent tunneling experiments [87] on incommensurate CDWs. There are also other cases of CDWs where conducting chains are modulated by counterion columns. One is the very first known CDW compound, the Pt chain KCP - in the stoichiometric version  $\text{K}_{1.75}[\text{Pt}(\text{CN})_4]1.5\text{H}_2\text{O}$ . It was shown theoretically [88], with an interpretation of available experimental data, that the "weak two-fold commensurability" induced by columns of counterions gives rise to the physics of phase  $\pi$  solitons. The mechanism of spinless conduction by the e-charged  $\pi$ -solitons might be universal to all systems with the charge ordering, irrespective to the ordering pattern. Actually the  $\pi$ -soliton is a 1D vision of a vacancy or an addatom in the Wigner crystal, which is the most universal view of the charge ordering. We shall return to this topics in the Sect. 6.2.

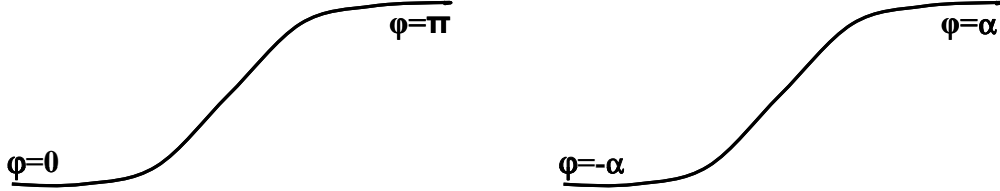


Figure 13: Phase profiles  $\varphi(x)$  of charged solitons. Left:  $\pi$  solitons = (anti)holons; spinless charge  $\pm e$  particles seen in conductivity. Right:  $\alpha$  solitons = domain walls of the ferroelectric polarization, seen in dispersion of the permittivity.

### 5.1.2 Ferroelectric solitons.

In the charge ordered phase,  $U_s \neq 0$  gives rise to the ferroelectric ground state, if the same  $\alpha$  is chosen for all stacks. The state is the two-sublattice AFE if  $\alpha$  signs alternate as in the  $(\text{TMTTF})_2\text{SCN}$ , and more complex patterns of  $\alpha$  are possible as it has been found in new compounds [31].

Spontaneous  $U_s$  itself can change the sign between different domains of ferroelectric displacements. Then the electronic system must also adjust the mean value of  $\varphi$  in the ground state from  $\alpha$  to  $-\alpha$  or to  $\pi - \alpha$ . Hence the ferroelectric domain boundary  $U_s \Leftrightarrow -U_s$  requires for the phase  $\alpha$ -solitons, Fig. 13, of the increment  $\delta\varphi = -2\alpha$  or  $\pi - 2\alpha$ , whichever is smaller; it will concentrate the non integer charge  $q$ :  $q/e = -2\alpha/\pi$  or  $q/e = 1 - 2\alpha/\pi$  per chain.

Above the 3D ordering transition  $T > T_{\text{CO}}$ , the  $\alpha$ -solitons can be seen as individual particles, charge carriers. Such a possibility requires for the fluctuational 1D regime of growing charge

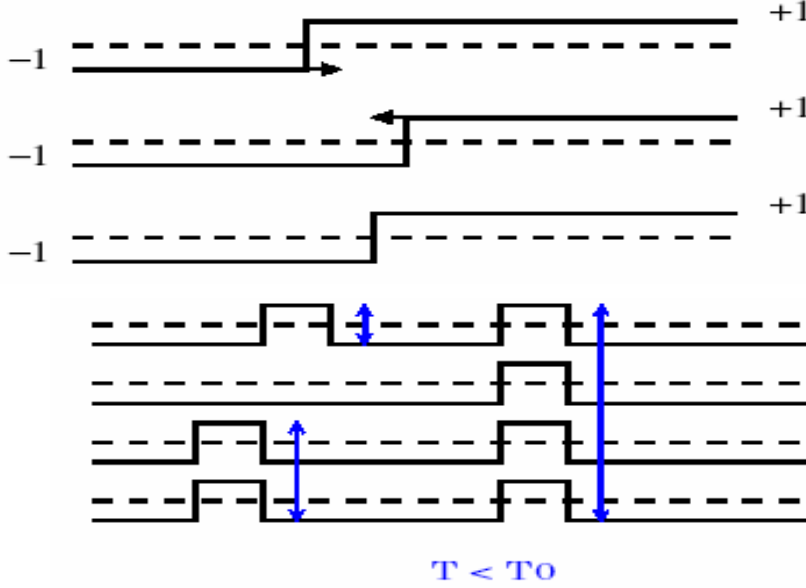


Figure 14: Crossover from on-chain ferroelectric solitons into ferroelectric domain walls at  $T < T_{CO}$ . Upper three lines: aggregation of solitons into the wall. Lower three lines: binding of solitons into pairs with subsequent aggregation into the bubble - the nucleus of the opposite polarization. After [89].

ordering. It seems to be feasible in view of a strong increase of  $\varepsilon$  at  $T > T_{CO}$  even for the AFE case of the X = SCN in Fig. 6, which signifies the growing single chain polarizability before the 3D interactions enter the game.

Below  $T_{CO}$ , the  $\alpha$ - solitons must be aggregated into domain walls [89], separating domains of opposite ferroelectric polarization. The noticeable asymmetry in the frequency dependence of  $\varepsilon'$  above and below  $T_{CO}$ , Fig. 8, might be just due to this aggregation. The nonsymmetry shows up much stronger in the frequency dependence of the imaginary part of the permittivity  $\varepsilon''$ , see figures in [48, 26, 49]. The peak in  $\varepsilon''(\omega)$  determines the relaxation time  $\tau$  showing two temperature regimes:

- 1) Near  $T_{CO}$ ,  $\tau(T)$  grows sharply corresponding to the expected slowing down of the critical collective mode;
- 2) At low  $T$ ,  $\tau$  grows exponentially following the activated law with the energy similar to the one of the conductivity,  $\Delta$ ; hence the relaxation is external, via resistance of the electrically coupled gas of charge carriers -  $\pi$ - solitons.
- 3) Below the main peak in  $\varepsilon''(\omega)$ , a long tail appears at  $T < T_{CO}$ , showing a weak secondary maximum. This tail may be well interpreted as the internal relaxation of the ferroelectric polarization through the motion of pinned domain walls - aggregated  $\alpha$ - solitons.

## 5.2 Effects of subsequent transitions:

### Spin-charge reconfinement and combined solitons.

Physics of solitons is particularly sensitive to a further symmetry lowering, and the subsequent anion ordering of the tetramerization in  $(\text{TMTTF})_2\text{ReO}_4$  [15, 25, 24] is a very fortunate example. This true present from the Nature demonstrates clearly the effect of the spin-charge reconfinement. Similar effects are expected for the Spin-Peierls state, e.g. in  $(\text{TMTTF})_2\text{PF}_6$ , but the clarity of the 1D regime in  $\text{ReO}_4$  is uniquely suitable to keep the physics of solitons on the scene.

The conductivity plot for the  $\text{ReO}_4$  case in Fig. 10 shows, at  $T=T_{AO}$ , the jump in  $\Delta$  (actually even in  $G(T)$ , see details in [25, 26]) which is natural for the first order transition. We argue that the new higher  $\Delta$  at  $T < T_{AO}$  comes from special topologically coupled solitons which explore both the charge and the spin sectors.

Now we must invoke also the phase  $\theta$  describing the spin  $\sigma$  degree of freedom, such that  $\theta'/\pi$  is the smooth spin density. Its free distortions are described by the Hamiltonian

$$H_\theta = \frac{1}{4\pi} \{ (\partial_x \theta)^2 v_\sigma + (\partial_t \theta)^2 / v_\sigma \} \quad (3)$$

where  $v_\sigma \sim v_F$  is the spin sound velocity. (The absence of the factor  $\gamma^{-1}$  in 3 in comparison with (1) is not a typing mistake.)

The additional deformation of tetramerization, Fig. 15, acts upon electrons as a  $2K_F$  CDW, Fig. 11- right panel, thus adding the energy

$$H_V = -V \cos(\varphi - \beta) \cos \theta \quad (4)$$

(Here the shift  $\beta$ , mixing of site and bond distortions, reflects the lack of the inversion symmetry, since  $T_{AO}$  is already below  $T_{CO}$ .) Within the reduced symmetry of Fig. 15, the invariant Hamiltonian becomes

$$H_U + H_V = -U \cos(2\varphi - 2\alpha) - V \cos(\varphi - \beta) \cos \theta \quad (5)$$

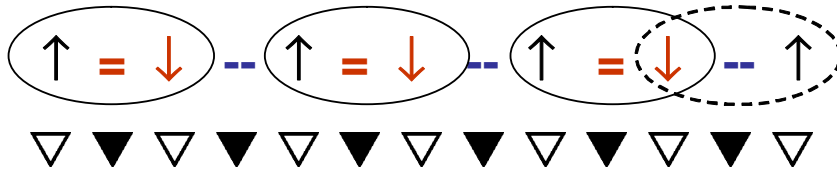


Figure 15: Effect of the tetramerization leading to the energy (4). White and black triangles show the site inequivalence after the charge ordering. Tetramerization adds the inequivalence of spin-exchange bonds = and -. Ellipses show the preferable spin singlets. The last dashed ellipse shows an alternative spin configuration which was equivalent above the  $T_{AO}$ ; now, at  $T < T_{AO}$ , it becomes the spin excitation.

Fig. 15 suggests a schematic illustration for the effect of the tetramerization. Inequivalence of bonds = and - between good sites endorses ordering of spin singlets. Also it prohibits translation by the two-site distance which was explored by the  $\delta\varphi = \pi$  soliton. But its combination with

the soliton ( $\delta\theta = \pi$ , which shifts the sequence of singlets) carrying the unpaired spin, is still allowed as the selfmapping.

Formation at  $T < T_{AO}$  of the new V-term (4) destroys the spin liquid, which existed at  $T > T_{AO}$  on top of the charge ordered state. The V term in (5) lifts the continuous  $\theta$ - invariance, thus opening at  $T < T_{AO}$  the spin gap  $\Delta_\sigma \sim V^{2/3}$ , as it is known for the spin-Peierls transitions [90, 92]. Moreover, it lifts even the discrete invariance  $\varphi \rightarrow \varphi + \pi$  of  $H_U$ , thus prohibiting the  $\pi$  solitons to exist alone; now they will be confined in pairs (either neutral or  $2e$  - charged) tightened by spin strings. But the joint invariance

$$\varphi \rightarrow \varphi + \pi, \theta \rightarrow \theta + \pi$$

is still present in (4), giving rise to *compound topological solitons* [91] (cf. [92]).

The major effects of the tetramerization V-term are the following:

a) to open the spin gap  $2\Delta_\sigma$  corresponding to creation of new  $\{\delta\theta = 2\pi, \delta\varphi = 0\}$  uncharged spin-triplet solitons,

b) to prohibit former  $\delta\varphi = \pi$  charged solitons, the holons, – now they are confined in pairs bound by spin strings, the activation  $\gtrsim 2\Delta$  is required.

c) to allow for topologically bound spin-charge compound solitons  $\{\delta\varphi = \pi\}$ ,  $\delta\theta = \pi$ , which leave the Hamiltonian (5) invariant, the activation  $\gtrsim \Delta$  is required.

For the last compound particle (c), the quantum numbers are as for a normal electron: the charge  $e$  and the spin  $1/2$ , but their localization is very different, Fig. 16. The compound soliton is composed with the charge  $e$  core soliton (here  $\delta\varphi = \pi$  within the shorter length  $\xi_\rho \sim \hbar v_F/\Delta$ ) which is supplemented by spin  $1/2$  tails of the spin soliton (here  $\delta\theta = \pi$  within the longer length  $\xi_\sigma \sim \hbar v_F/\Delta_\sigma \gg \xi_\rho$ ). This complex of two topologically bound solitons gives the carriers seen at  $T < T_{AO}$  at the conductivity plot for the  $X = \text{ReO}_4$ , Fig. 10 and [24].

Similar effects should take place below intrinsically electronic transitions, particularly relevant can be the spin-Peierls one for  $X = \text{PF}_6$ . But there the physics of solitons will be shadowed by  $3D$  electronic correlations, which are not present yet for the high  $T_{AO}$  of  $X = \text{ReO}_4$  case.

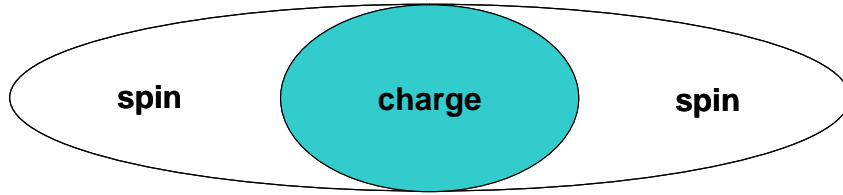


Figure 16: Illustration of confinement below the tetramerization transition. Different scales of spin and charge distributions within the compound solitons: charge  $e$ ,  $\delta\varphi = \pi$  is concentrated sharply within  $\xi_\rho \sim \hbar v/\Delta$ ; spin  $1/2$ ,  $\delta\theta = \pi$  is concentrated loosely within  $\xi_\sigma \sim \hbar v/\Delta_\sigma$ .

## 6 Optics

### 6.1 Optics: collective and mixed modes.

#### 6.1.1 Optics: phase mode.

Beyond the ferroelectric phase (e.g. the AFE state, or the disordered one at  $T > T_{CO}$ ) the optical absorption starts at the frequency  $\omega_t < 2\Delta$ , which is the bottom of the spectrum of

phase excitations  $\omega^2 = (v_\rho k)^2 + \omega_t^2$ . In the quasi-classical limit of small  $\gamma \ll 1$ ,  $\omega_t$  can be interpreted as the frequency of phase oscillations of the  $4K_F$  CDW around the minimum of the commensurability energy (3). The renormalized value  $U^*$  of  $U$  in (3) can be expressed through this observable parameter as

$$U^* = \frac{\omega_t^2}{8\pi\gamma v_\rho}, \quad \omega_t \approx \pi\gamma\Delta < \Delta \quad (\gamma \ll 1) \quad (6)$$

As a "transverse" frequency of the optical response,  $\omega_t$  gives the background dielectric susceptibility:

$$\varepsilon_\Delta(\omega) = \frac{\omega_p^{*2}}{(\omega_t^2 - \omega^2)}, \quad \omega_p^{*2} = \gamma \frac{v_\rho}{v_F} \omega_p^2, \quad \omega_p^2 = 8 \frac{e^2 v_F}{\hbar s} \quad (7)$$

where  $\omega_p^*$  and  $\omega_p$  are the actual plasma frequency of the parent metal and its bare value,  $s$  is the area per stack. In exact theory of the quantum sine-Gordon model,  $\omega_t$  appears as the first bound state  $E_1$  of the pair of solitons, see [95, 96, 97]. Its exact relation to the gap  $2\Delta$  is  $\omega_t = E_1 = 2\Delta \sin(\pi\tilde{\gamma}/2)$  as explained below in Eq.(9).

### 6.1.2 Optical permittivity $\varepsilon(\omega)$ near the ferroelectric transition.

We shall present, without derivation, the formula for the mixed electron-phonon contribution to the permittivity, valid at  $T \geq T_{CO}$  - above and approaching the ferroelectric transition:

$$\frac{\varepsilon(\omega)}{\varepsilon_\infty} = 1 + \frac{(\omega_p^*/\omega_t)^2(1 - (\omega/\omega_0)^2)}{(1 - (\omega/\omega_0)^2)(1 - (\omega/\omega_t)^2) - Z}, \quad Z = \left(\frac{\omega_{cr}}{\omega_t}\right)^{2-4\gamma} \leq 1 \quad (8)$$

Here  $\omega_0$  is a frequency of the molecular mode coupled to the charge ordering;  $\omega_{cr}(T)$  is the critical value of the collective mode frequency  $\omega_t(T)$ , below which the spontaneous ferroelectric charge ordering takes place. Near the critical point  $Z(T_{CO}) = 1$  we see here:

<i>Fano antiresonance</i>	at $\omega_0$ , just as observed in [69] - Fig. 17
<i>Combined electron-phonon resonance</i>	at $\omega_{0t}^2 \approx \omega_0^2 + \omega_t^2$
<i>FE soft mode</i>	at $\omega_{fe}^2 \approx (1 - Z)(\omega_0^{-2} + \omega_t^{-2})^{-1}$

Near  $T_{CO}$  the ferroelectric mode might be overdamped; then it grows in frequency following the order parameter, that is as  $\omega_{fe} \sim \varepsilon^{-1/2}$  (which can yield two orders of magnitude at low  $T$ ) to become finally comparable with  $\min\{\omega_0, \omega_t\}$ . Suggesting smooth  $T$  dependencies  $\omega_t(T)$  and  $\omega_{cr}(T)$ , we find the critical singularity at  $\omega = 0$  as  $\varepsilon(T) = A|T/T_{CO} - 1|^{-1}$ . It develops upon the already big gapful contribution  $A \sim (\omega_p^*/\omega_t)^2 \sim 10^3$  in agreement with experimental values  $\varepsilon \sim 10^4 T_{CO}/(T - T_{CO})$ . All that confirms that the ferroelectric polarization comes mainly from the electronic system, even if the corresponding displacements of ions are very important to choose and stabilize the long range  $3D$  order.

## 6.2 Optics: solitons.

Thanks to detailed information on the sine-Gordon model, we can clearly formulate the expectations for optical properties related to physics of solitons (see details in [95], and [96] for a review; the contemporary stage and comparison of different approaches can be found in [97]).

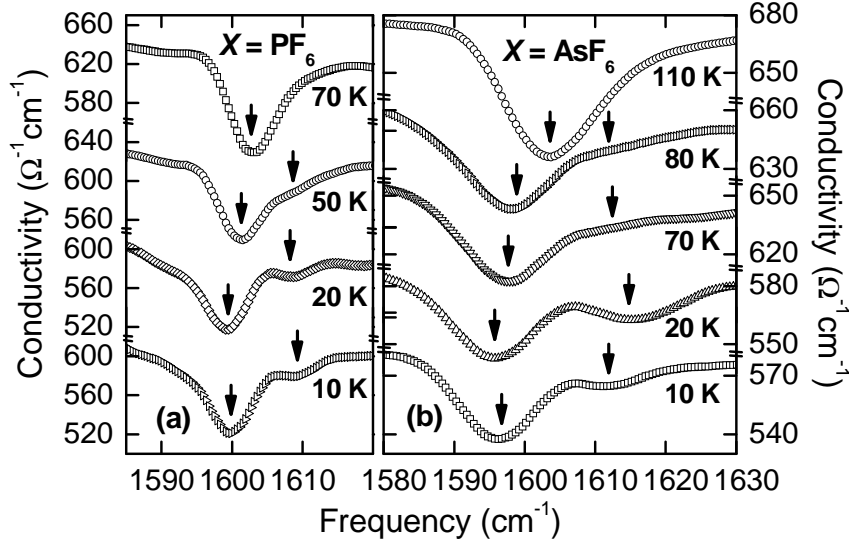


Figure 17: CO effect upon the molecular mode. The figure demonstrates two effects: 1) Fano antiresonance at any  $T \geq T_{CO}$  which might be due the stack polarizability; 2) its splitting at  $T < T_{CO}$  due the CD - in accordance with the NMR. After [69].

The most general feature of the optical spectra, valid through the whole gapful regime  $\gamma < 1$ , is the two-particle gap  $E_g = 2\Delta$  corresponding to the creation of a pair of  $\pm\pi$  solitons. Contrary to the common sense intuition and the elementary theory, the absorption  $I(\omega)$  has no singularity at the threshold  $E_g$ . The optical density of states law  $DOS \sim (\omega - E_g)^{-1/2}$  is compensated by vanishing of the matrix element. As a result, the absorption starts smoothly as  $I \sim (\omega - E_g)^{1/2}$ . Realistically, the gap will be seen only as the nonsingular threshold for the photoconductivity, where other absorption mechanisms are excluded. For the built-in Mott state without the charge ordering,  $1/2 < \gamma < 1$ , there is no absorption below  $E_g$ . This case was studied in detail in [98].

But for the Mott state due to the spontaneous charge ordering,  $\gamma < 1/2$ , there might be also sharp peaks of the optical absorption even below the two-particle gap  $E_g = 2\Delta$ . Actually the spectral region  $\omega < 2\Delta$  is filled by a sequence of quantum breathers, bound states of two solitons at energies

$$E_n = 2\Delta \sin\left(\frac{\pi}{2}\tilde{\gamma}n\right), \quad \tilde{\gamma}^{-1} = \gamma^{-1} - 1. \quad (9)$$

Here the substitution of  $\gamma$  for  $\tilde{\gamma}$  takes into account quantum corrections to the control parameter itself [96]. The modes with odd numbers  $n$  are optically active. The primary, lowest bound state  $E_1$  gives the corrected value for the collective mode  $\omega_t$ . It reduces to the classical result of (6) in the limit of small  $\gamma \ll 1$ , where  $E_1 = 2\Delta \sin(\pi/2\tilde{\gamma}) \approx \pi\gamma\Delta = \omega_t < 2\Delta$ .

At a sequence of special values of  $\gamma_n = 1/2n$ , starting from  $\gamma = 1/2$  downwards, the next bound state splits off from the gap. Only at these moments, the absorption edge singularity blows up from the smooth dependence  $\sim (\omega - E_g)^{1/2}$  to the divergency  $DOS \sim (\omega - E_g)^{-1/2}$ . (There is a crossover near these values of  $\gamma$  [97], where a rounded edge singularity can be observed.) This property opens an amusing possibility to observe spectral anomalies at special values of the monitoring parameter, varying it e.g. by applying pressure.

We see that the scheme changes qualitatively just at the borderline for the charge ordering instability  $\gamma = 1/2$ : from the essentially quantum regime  $1/2 < \gamma < 1$  (with  $E_g = 2\Delta$  and



no separate  $\omega_t$  at all) to the quasi classical low  $\gamma$  regime with a sequence of peaks between  $2\Delta$  and  $\omega_t$ . This fact was not quite recognized in existing interpretations, see [82], of intriguing optical data [93, 99, 100]. E.g. the detailed theoretical work [98] was all performed for the case equivalent to  $\gamma > 1/2$ , in our notations, and cannot be applied to the  $(\text{TMTTF})_2\text{X}$  case as it was supposed. The studies of [95] and [97] are quite applicable, with the adjustment to the two-fold commensurability, which we have implied above.

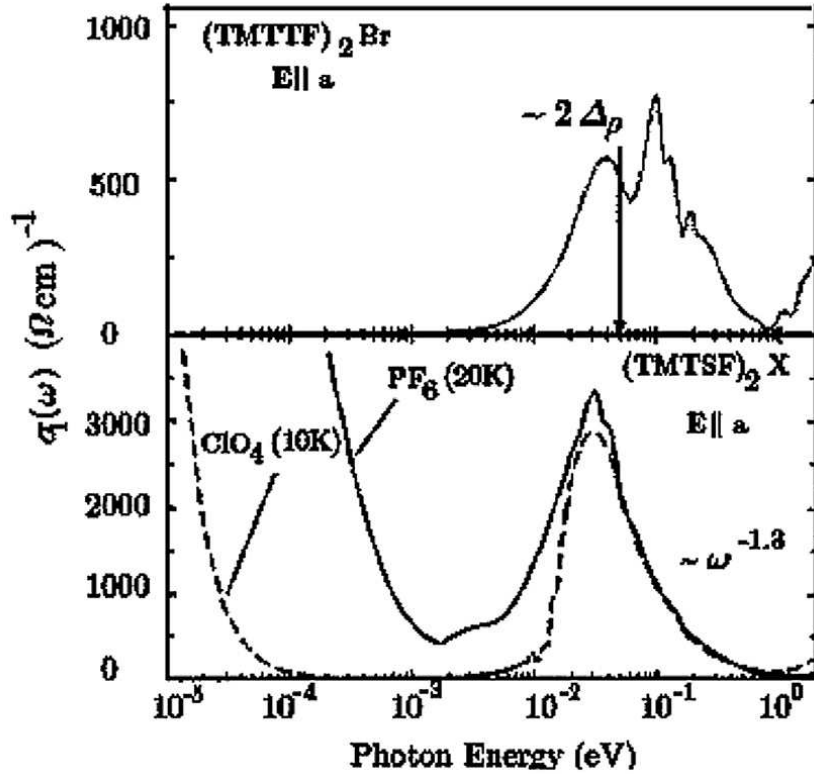


Figure 18: Comparison of optical absorption of TMTTF and TMTSF compounds in a wide  $\omega$  range. It seems that after subtracting molecular peaks at the high  $\omega > 2\Delta_\rho$  slope (upper panel) the gaps shapes will be quite similar in both TMTTF and TMTSF cases. Is it a way to prove the hidden charge ordering in the metallic state of the Se subfamily? After [93]

The available experiments, see Figs. 18 and 19, can be interpreted as observations of the collective mode - solitons' bound state. Photoconductivity experiments (distinguished from the bolometric effect !) are necessary to discriminate between two absorption mechanisms: at  $\omega_t$  and above  $2\Delta$ .

Recall that quenching of the edge singularity is not just a peculiar property of the sin-Gordon model. It takes place also in theory [101] of generic 1D semiconductors such as conjugated polymers, as a consequence of the final state interaction via the long range Coulomb forces. Merging of local and Coulomb interaction is still an unattended issue in theory of solitons.

### 6.3 Optics: summary.

Now we summarize shortly the main expected optical features [57].

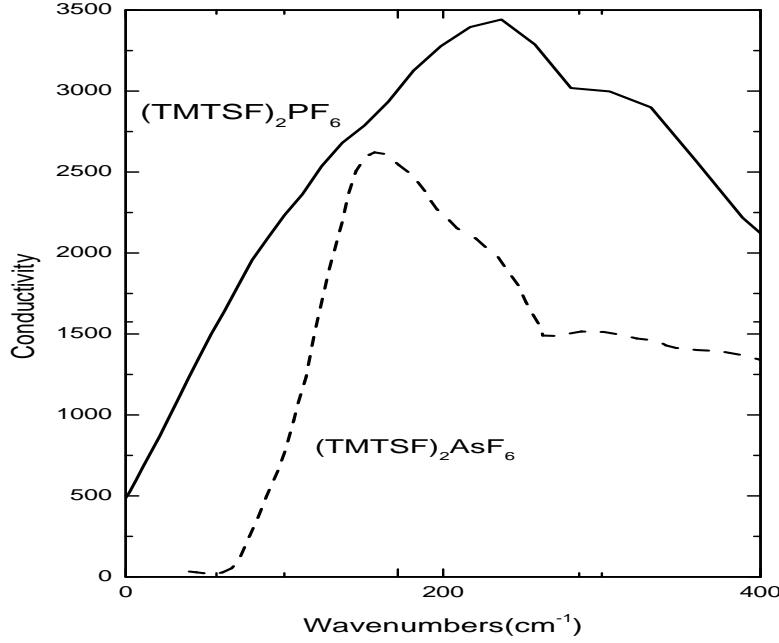


Figure 19: Optical spectra of two  $(\text{TMTSF})_2\text{X}$  salts. The case of  $\text{AsF}_6$  shows a clear excitonic peak which may be the mode  $\omega_t$ . The case of  $\text{X} = \text{PF}_6$  shows a more smeared feature, probably due to the noticeably high SDW gap within the charge ordering one. The shoulders seen at frequencies above the peaks can be well interpreted as the two-particle gaps  $2\Delta$ . Then they will determine the thresholds in photoconductivity. M. Dressel, unpublished.

**I.** In any case of the CO, for both FE or AFE orders, we expect

- Ia) Strongest absorption feature comes from the phase mode, an analogy of the exciton as the bound kink-antikink pair at  $\omega_t$ ;
- Ib) Two-particle gap  $2\Delta$  (e.g. the photoconductivity) lies higher than  $\omega_t$ , it is given by free pairs of  $\pi$ -solitons,  $\Delta = E_\pi$ ;
- Ic) Spectral region  $\omega_t < \omega < 2\Delta$  may support also quantum breathers – higher bound states of solitons.

**II.** In case of the ferroelectric order we expect additionally or instead of I:

- IIa) Fano antiresonance at the bare phonon mode frequency  $\omega_0$  coupled to the CO;
- IIb) Combined electron-phonon resonance at  $\omega_{0t} > \omega_0, \omega_t$ , which substitutes for Ia;
- IIc) Ferroelectric soft mode at  $\omega_{fe}$ , evolving from  $\omega_{fe} = 0$  at  $T < T_{\text{CO}}$ .

Unfortunately, the optical picture of  $(\text{TMTTF})_2\text{X}$  compounds is complicated by multiple phonon lines filling just the relevant region of the optical gap. But this complication may not be all in vain, if it is viewed also as another indication for the charge ordering. Indeed, surprisingly (kept noticed since early 80's [102]) high intensity of molecular vibrations in TMTTF may be

just due to the inversion symmetry lifting by the charge ordering, recall [103] for well confirmed mechanisms of phonons activation by the CDW formation. Oppositely, weaker phonon lines in TMTSF [102] may speak in favor of a fluctuational regime of the charge ordering in accordance with the pseudogap, rather than a true gap, in electronic optical transitions.

The whole obstacle can be overcome by experiments on low gap charge ordered states like in (TMTTF)<sub>2</sub>Br, or under pressure. There, as one can guess from other experiments [104, 105], the gap value will fall below the region of intensive molecular vibrations, which today prevent the observations. Fig. 18 shows that it is happening indeed, and just for X=Br as expected: the electronic spectrum starts to split off from the vibrational one.

Recall finally the great experience of optics in another type of strongly correlated 1D electronic systems: conjugated polymers. They were studied by such a complex of optical techniques as photoconductivity, stimulated photoemission, photoinduced absorption, electro-absorption, time resolved measurements, see refs. in [106].

A popular interpretation (see [82] for a review) of optics [93, 99, 100] and sometimes conductivity [22] in TMTCF - type compounds neglects the dimerization (either generic from bonds or from sites via the charge ordering) and relies upon the weaker 4- fold commensurability effects. They give rise to the energy  $\sim U_4 \cos 4\varphi$  originated by higher order (8 particles collisions) Umklapp processes; its stabilization would require a stronger  $e - e$  repulsion (or slowing down, see Sect. 8.1) corresponding to  $\gamma < 1/4$ . While not excluded in principle, this mechanism does not work in TMTTF case, already because this scenario does not invoke any charge ordering instability. Moreover, the experiment shows, Fig. 9, that even small increments of the dimerization, just below the second order transition at  $T_{CO}$ , immediately transfer to the activation energy, hence the domination of the two-fold commensurability.

## 7 Fate of the metallic TMTSF subfamily.

By now, the re-valuation definitely concerns mostly the TMTTF subfamily, whose members usually, by the temperature  $T_{CO}$ , already fall into the charge-gap regime starting at  $T_p > T_{CO}$ , see Fig. 9. The TMTSF compounds are highly conductive, which does not allow for measurements of the low frequency permittivity  $\epsilon$ . Also the NMR splitting [27, 107] will probably be either too small or broadened because of expected disordered or temporal nature of the charge ordering in the metallic phase (see [33] for a proved example of another system with the charge ordering). Nevertheless the transition may be there, just being hidden or existing in a fluctuation regime, as may be realized, e.g., in stripe phases of High- $T_c$  cuprates [108]. If and when confirmed, the entire picture of intriguing abnormal metallic state [109] will have to be revised following the TMTTF case.

The signature of the ferroelectric charge ordered state may have been already seen in optical experiments [93, 99, 100], as we have discussed above. Indeed, the Drude-like low frequency peak appearing within the pseudogap, Fig. 18 - lower panel, can be interpreted now as the optically active mode of the ferroelectric polarization; the joint lattice mass, see Sect. 8.1, will naturally explain its otherwise surprisingly low weight. Recall here the earlier conjectures on collective nature of the conductivity peak [12, 13, 110], derived from incompatibilities of IR optics, conductivity and NMR. Vice versa, the ferroelectric mode must exist in TMTTF compounds, whose identification is the ultimate goal. Even the optical pseudogap itself [93, 99, 100], being unexpectedly large for TMTSF compounds, Fig. 18-top, with their less pronounced

dimerization of bonds, can be largely due to the hidden spontaneous dimerization of sites. Even the shapes of the gap and the pseudogap in TMTTF and TMTSF cases appear to look similar, if the first one is cleaned from molecular modes, Fig. 18 - upper panel. Optical experiments will probably be elucidated when addressed to members of the (TMTTF)<sub>2</sub>X family, showing the charge ordering with a particularly reduced value of the associated gap (below typical molecular vibrations - down to the scale of the pseudogap in (TMTSF)<sub>2</sub>X).

Hidden existence of the charge ordering and the local ferroelectricity, at least in fluctuating regime, is the fate of the TMTSF compounds and the major challenge is to detect it, as it was seen explicitly in TMTTF compounds. Key effects of anion orderings, particularly the opportunity to compare relaxed and quenched phases of (TMTSF)<sub>2</sub>X, also are waiting for attention.

## 8 Origin and range of basic parameters.

### 8.1 Generic origins of basic parameters:

#### Interactions among electrons or with phonons?

The combination of optical and conductivity data can provide a deeper insight into the nature of observed regimes. The value of  $\Delta$  is already known as the conductivity activation and  $2\Delta$  can be found independently as the photoconductivity threshold;  $\omega_t$  is measurable through the optical absorption. Then their ratio will provide the basic microscopic parameter  $\gamma$ .

The full quantitative implementation requires to resolve for divergence (2,3 or even more times !) [100, 102] in values of such a basic and usually robust parameter as the plasma frequency, if it is extracted from different parts of the spectrum. This discrepancy can signify the strong renormalization  $\omega_p^* \ll \omega_p$ , which can develop while the probe frequency decreases from the bare scale  $\omega_p > 1\text{eV}$  to the scale  $\omega_t, \omega_0 \sim 10^{-2}\text{eV}$ .

Remind the full (kinetic  $\sim C_{kin}$  and potential  $\sim C_{pot}$ ) energy of elastic deformations for the charge phase  $\varphi$ :

$$\frac{\hbar v_F}{4\pi} \{ (\partial_t \varphi)^2 C_{kin}/v_F^2 + (\partial_x \varphi)^2 C_{pot} \} \equiv \frac{1}{4\pi\gamma} \{ (\partial_t \varphi)^2/v_\rho + (\partial_x \varphi)^2 v_\rho \}$$

where

$$\gamma = \frac{1}{C_{pot}C_{kin}}, \quad \frac{v_\rho}{v_F} = \frac{C_{pot}}{C_{kin}}, \quad \frac{\omega_p^*}{\omega_p} = \left( \gamma \frac{v_\rho}{v_F} \right)^{1/2} = \frac{1}{C_{kin}}$$

The potential parameter  $C_{pot}$  is "1+ e-e repulsion contribution". The kinetic parameter  $C_{kin}$  is "1+lattice adjoined mass". The parameter  $\gamma$  contains a product of C's – not distinguishable separately; the velocity  $v_\rho$  contains a ratio of C's – not distinguishable separately. But  $\omega_p^*$  contains only  $C_{kin}$ , which gives a direct access to the joint lattice dynamics. (Another factor for reduction of the parameter  $\gamma$ , the Coulomb hardening  $C_{pot} > 1$ , acts upon  $\gamma$  and velocity  $v_\rho$ <sup>11</sup>, but cancels in their product which gives  $\omega_p^*$ .) The lowering of  $\omega_p^*$  singles out the effect of the effective mass enhancement  $C_{kin} > 1$ , which is due to coupling of the charge ordering with  $4K_F$  phonons [113]<sup>12</sup>.

---

<sup>11</sup>In CDWs the Coulomb hardening, as well as the very common mass enhancement [112], are confirmed experimentally [111]

<sup>12</sup>X-ray scattering gives a direct evidence for the coupling of the  $4K_F$  electronic density with either lattice displacements [37, 38, 40] or intramolecular modes [114].

The final step is to notice that the mass enhancement will not be effective above the  $4K_F$  phonon frequency  $\omega_{ph}$ ; actually  $C_{kin}$  is a function of  $\omega$ :  $C_{kin}(\omega) = C_{kin}(0)\omega_{ph}^2/(\omega_{ph}^2 + \omega^2)$ . It explains the difference in values of  $\omega_p^*$  extracted from high and from intermediate frequency ranges. If true, then the charge ordered state is a kind of a polaronic lattice (as it was already guessed for some CDWs [115]). It resembles another Wigner crystal: electrons on the liquid Helium surface, see [116], where selftrapped electrons gain the effective mass from surface deformations - the ripples.

## 8.2 Where are we?

There are still several fascinating questions to understand:

Why the charge ordering is so common and appears at such a high energy/temperature scale?

Why do we see it instead of the abnormal metal (Luttinger Liquid regime)?

Why does it develop spontaneously before the 1/4 filling effects have a chance to be seen?

We may get an idea for the answers to these questions by analyzing the sequence of various regimes, as it appears by changing the control parameter  $\gamma$ .

Phenomenological Hamiltonian may have the following typical components (we restrict it here to terms containing only the charge phase  $\varphi$ ).

$$H_\varphi \sim \gamma^{-1}[v_\rho(\partial_x \varphi)^2 + v_\rho^{-1}(\partial_t \varphi)^2] -$$

from the electron liquid or fluctuating  $4K_F$  CDW (**basic**)

+  $U_1 \cos(\varphi)$  – from tetramerization or spin-Peierls (**spontaneous, frequent**)

+  $U_2 \cos(2\varphi)$  – from dimerization (**built-in or spontaneous, typical**)

+  $U_3 \cos(3\varphi)$  – from trimerization: TTF-TCNQ under pressure,

NMP-TCNQ (**special**)

+  $U_4 \cos(4\varphi)$  – built-in, from host lattice (**typical**).

The parameter  $\gamma = K_\rho$  controls quantum fluctuations of the phase  $\varphi$  which will, or will not, destroy the above nonlinearities; it defines:

1. survival, against renormalization to zero, of nonlinearities  $\sim U_i$ ;
2. their spontaneous generation – known for  $U_1, U_2$ ;
3. physics of solitons and the collective mode;
4. relevance of the interchain coupling: metal/insulator branching.

We can quote the following regimes.

$\gamma < 1$  : Renormalized  $U_2 \neq 0$ ; the charge gap is originated in case of built-in dimerization (of either bond or site types). This is the generic Mott-Hubbard state, any repulsion is sufficient to stabilize it. Solitons = holons appear as free excitations, giving both the thermal activation energy in conductivity, and the optical absorption threshold. This regime is certainly valid for all (TMTTF)<sub>2</sub>X. It is not applicable to nondimerized materials like DMtTTF and EDT-TTF-CONMe salts [30, 78]. They still would be metallic, unless falling into the next regime described below, which does happen actually.

$\gamma < 1/2 = 0.5$  :  $4K_F$  anomaly appears in X-ray scattering at high T, as registered in fractionally filled cases of TTF-TCNQ and its derivatives [40, 38, 41]. In 1/4 filled compounds the spontaneous site dimerization potential  $\sim U_s$  is formed, hence no need for a bare commensurability/umklapp potential  $\sim U_b$ . This regime is proved to be valid, by observations of the ferroelectric response and the NMR splitting, in most of TMTTF<sub>2</sub>X, and by X-rays [31] in

(DMtTTF)<sub>2</sub>ClO<sub>4</sub>.<sup>13</sup> All materials are waiting for determining the optical signatures, see Sect. 6.3.

$\gamma < 4/9 = 0.39$  : Trimerization lock-in of  $4K_F + 2K_F$  superlattices (confirmed in TMTTF-TCNQ under a special pressure [42] and in NMP-TCNQ [41]).

$\gamma < 1/4 = 0.25$  : effects of 1/4 filling may come to play (cf. the lock-in of sliding of CDWs under stress in MX<sub>3</sub> conductors [117, 118]).

$\gamma < \sqrt{5} - 2 \approx 0.24$  : ultimate SDW instability, even for incommensurate cases. (The confinement index of the electron pair in the course of the interchain hopping is  $(1/\gamma - \gamma)/2 < 2$  [17, 18]). Seemingly, it is not the case of TMTSF metals: they need the HMF support to form the FISDW.

$\gamma \approx 0.23$  : a guess from high  $\omega \gg \Delta$  tails ( $\sim \omega^{-1/3}$ , see Fig. 18) of optical absorption [99], see also [82].

$\gamma < 2/9 \approx 0.22$  : spontaneous trimerization which is not observed: TTF-TCNQ needs a precise pressure to pinpoint exactly 1/3.

$\gamma < 3 - \sqrt{8} \approx 0.17$  : last feature of electrons' Fermi surface disappears. (The electron Green function index is  $(\gamma + 1/\gamma + 2)/4 < 2$ .) This regime was guessed from ARPES experiments in (TMTSF)<sub>2</sub>X [119], but not seen in seemingly more correlated TTF-TCNQ [120].

$\gamma = 0.125$  : spontaneous 1/4 filling in totally incommensurate chains. But the usual CO, the  $4K_F$  condensation, would have happened already well before.

*Resume:* most of qualitative effects of electronic correlations would appear at  $\gamma < 1/2$ , where the system is already unstable with respect to the charge ordering. The existing experiments on most studied materials pose the following constraints. (TMTTF)<sub>2</sub>X :  $\gamma < 0.5$ ; (TMTSF)<sub>2</sub>X :  $\gamma > 0.24$ ; TTF-TCNQ :  $0.22 < \gamma < 0.39$ .

## 9 Conclusions and perspectives.

We have presented the key issues of related phenomena of the Ferroelectricity and the Charge Ordering in organic metals. In (TMTTF)<sub>2</sub>X the dielectric permittivity  $\varepsilon$  demonstrates clear cases of the ferroelectric and anti-ferroelectric phase transitions. The combination of conductivity and magnetic susceptibility proves the spinless nature of charge carriers. The independence and occasional coexistence of structureless ferroelectric transitions and usual anionic ones brings the support of structural information. The sequence of symmetry breakings gives access to physics of three types of solitons:  $\pi$ - solitons (holons) are observed via the activation energy  $\Delta$  in conductivity; noninteger  $\alpha$ - solitons (ferroelectric domain walls) provide the low frequency dispersion; topologically coupled compound spin-charge solitons determine the conductivity below a subsequent structural transition of the tetramerization. The photoconductivity gap  $2\Delta$  will be given by creations of soliton - antisoliton pairs. The lower optical absorption comes from the collective electronic mode: in the ferroelectric case it becomes the mixed electron-phonon resonance coexisting with the Fano antiresonance. The ferroelectric soft mode evolves from the overdamped response at  $T_{CO}$ . The reduced plasma frequency signifies the slowing down of electrons' collective motion by the adjoint lattice mass; it recalls that the charge ordering has a  $4K_F$  lattice counterpart in accordance with the X-ray experience [37].

---

<sup>13</sup>The last compound, as well as (EDT - TTF - CONMe)<sub>2</sub>X, is still waiting for the standard (ferroelectricity, NMR) characterization.

We propose that a latent charge ordering in the form of ferroelectricity exists even in the Se subfamily  $(\text{TMTSF})_2\text{X}$ , giving rise to the unexplained yet low frequency optical peak and the enhanced pseudogap. Another, interchain type of the charge disproportionation, known in the relaxed  $(\text{TMTSF})_2\text{ClO}_4$ , is still waiting for attention; possibly it is present, perhaps also in a hidden form, in other superconducting cases. Discoveries of the ferroelectric anomaly and of the related charge ordering call for a revaluation of the phase diagram of the  $(\text{TMTTF})_2\text{X}$  and similar compounds and return the attention to the interplay of electronic and structural properties. In this respect, we point to the old theory [17, 18] for the synergetic phase diagram of these materials.

The ferroelectricity discovered in organic conductors, beyond its own virtues, is the high precision tool to diagnose the onset of the charge ordering and the development of its order. The wide range of the ferroelectric anomaly ( $T_{\text{CO}} \pm 30\text{K}$ ) suggests that the growing charge ordering dominates the whole region below and even above these already high temperatures. Even higher is the on-chain energy scale, from 500K up to 2000K, as given by the conduction gaps formed at lower T, and by optical features. Recall also the TTF-TCNQ with ever present, up to the RT,  $4K_F$  fluctuations. All that appears at the "Grand Unification" scale, which knows no differences with respect to interchain couplings, anion orderings, ferro- and antiferroelectric types, between Sulphur and Selenium subfamilies, between old faithful incommensurate or weakly dimerized compounds and the new quarter-filled ones. Hence the formation of the Electronic Crystal (however we call it: *disproportionation, ordering, localization or Wigner crystallization of charges;  $4K_F$  density wave, etc.*) must be the starting point to consider lower phases and the frame for their properties.

On the theory side, the richness of symmetry-defined effects of the charge ordering, ferroelectricity, AFE and various AOs (see [17, 18] for earlier stages) allows for efficient qualitative assignments and interpretations.

Still there are standing questions on charge ordering and ferroelectricity:

Why is the charge ordering so common?

Is it universal?

Why is the astonishing ferroelectricity so frequently encountered

as a form of charge ordering?

Why do the AFE and more complex patterns appear on other occasions?

Is it a spontaneously created Mott-Hubbard state?

Is it a Wigner crystal, if yes then of what: electrons or polarons?

Is it a  $4K_F$  CDW: driven by electrons and stabilized by the lattice?

Role of anions: is there a key to the FE/AFE choice?

Are there other challenges ignored since decades? Examples: the plasma frequency mystery, the special anion ordering structure for superconducting phase.

The last remark reminds us that the story of hidden surprises may not be over. Another, interchain, type of the charge disproportionation, known in the relaxed  $(\text{TMTSF})_2\text{ClO}_4$  (see more in [15]), is still waiting for attention, possibly being present in a latent form in other superconducting cases. This additional anion ordering can contribute to the controversial physics of inhomogeneous state at the SC/SDW boundary under pressure (see Chaikin, Jérôme, Heritier, et al in this volume). The coexistence of charge ordering and anion ordering transitions in  $(\text{TMTTF})_2\text{ReO}_4$  warns for this possibility in other cases as well. If it is not found to be the case, then we will be forced to accept two different types of superconductivity in  $(\text{TMTSF})_2\text{ClO}_4$  and in  $(\text{TMTSF})_2\text{PF}_4$  under pressure; the state of today's theories [81] still ignores the challenges from this anion ordering.

We conclude with the overview of challenges for future studies:  
 hidden existence of charge ordering and ferroelectricity in the metallic *Se* subfamily;  
 optical identification of gaps and soft modes;  
 physics of solitons via conductivity, optics, NMR;  
 ferroelectric hysteresis, relaxation, domain walls;  
 more exploration of anion ordering and other structural information.

We finish to say that new events call for a substantial revision of the contemporary picture of the most intriguing family of organic metals and its neighbors, and for further efforts to integrate various approaches to their studies.

### Acknowledgments.

Author acknowledges collaboration with P. Monceau and F. Nad, discussions with S. Brown, H. Fukuyama, J.-P. Pouget and S. Ravy, comments from R. Ramazashvily and S. Teber.

## References

- [1] Proceedings of the ICSM 1982, R. Comès et al eds., J. Phys. France, Colloque C3, **44**, (1983).
- [2] Proceedings of the ISCOM 2001 (Yamada Conference), G. Saito ed., Synth. Met., **133-134** (2003).
- [3] Proceedings of ISCOM 2003, P. Batail, E. Canadell and N. Dupuis, et al eds., J. Physique IV, v. **114** (2004).
- [4] Proceedings of ISCOM 2005, J. Brooks ed., to be published.
- [5] Proceedings of the ICSM 2002, Synthetic Metals, C.Q. Wu, Y. Cao, X. Sun and D.B. Zhu eds., v. **135-137** (2003).
- [6] Proceedings of the ICSM 2004, L.A.P. Kane-Maguire and D.L. Officer eds., Synthetic Metals, v. **152** (2005).
- [7] Proceedings of ECRYS 2002, S. Brazovskii, N. Kirova and P. Monceau eds., J. Phys. France IV, **12** (2002).
- [8] Proceedings of ECRYS 2005, S. Brazovskii, N. Kirova and P. Monceau eds., J. Phys. France IV, v. **131** (2005).
- [9] Organic Conductors, J.P. Farges ed. (M. Dekker Inc., New York 1994).
- [10] Common Trends in Synthetic Metals and High- $T_c$  Superconductors (I.F. Schegolev memorial volume), S. Brazovskii ed., J. Physique I, **6**, (1996).
- [11] Electronic properties of inorganic Quasi 1D compounds, P. Monceau ed. (D. Reidel publ., 1985).
- [12] D. Jérôme in [9], p. 405.
- [13] D. Jérôme, Chem. Rev. **104**, 5565 (2004).



- [14] R. Moret, J.-P. Pouget, R. Comès and K. Bechgaard, in [1], p. 957.
- [15] J.-P. Pouget and S. Ravy, in [10], p. 1501.
- [16] V.J. Emery, in[1], p. 977.
- [17] S. Brazovskii and V. Yakovenko, J. Physique Lett., **46**, 111 (1985).
- [18] S. Brazovskii and V. Yakovenko, JETP **62**, 1340 (1985).
- [19] R. Laversanne, C. Coulon, B. Gallois et al, J. Physique. Lett. **45**, L393 (1984).
- [20] C. Coulon, S.S.P. Parkin and R. Laversanne, Phys. Rev. B **31**, 3583 (1985).
- [21] H.H.S. Javadi, R. Laversanne and A.J. Epstein, Phys. Rev. B **37**, 4280 (1988).
- [22] C. Coulon, in [3], p. 15.
- [23] P. Monceau, F. Nad and S. Brazovskii, Phys. Rev. Lett., **86**, 4080 (2001).
- [24] S. Brazovskii, P. Monceau and F. Nad in [5], p. 1331; **cond-mat**/0304483.
- [25] F. Nad, P. Monceau, C. Carcel et al, in [2], p. 265; F. Nad, in [7], p. 133.
- [26] F. Nad and P. Monceau, J. Phys. Soc. Japan (2006) to be publ.
- [27] D.S. Chow, F. Zamborszky, B. Alavi et al, Phys. Rev. Lett. **85**, 1698 (2000); S. Brown in [7, 2, 5]; F. Zamborszky, W. Yu, W. Raas et al, Phys. Rev. B **66**, R081103 (2002).
- [28] W. Yu, F. Zamborszky, B. Alavi et al, in [3], p. 35.
- [29] H. Seo, M. Ogata and M. Kuwabara, in [3], p. 29.
- [30] P. Batail in [8], p. 307
- [31] S. Ravy, P. Foury-Leylekian, D. Le Bolloc'h, et al, in [3], p. 81.
- [32] H. Fukuyama, in [2], p. 257 and in [5], p. 673.
- [33] T. Takahashi, K. Hiraki, S. Moroto, et al, in [8], p. 133.
- [34] F. Nad and P. Monceau at ECRYS 2005 [8], unpublished.
- [35] H. Matsui, H. Tsuchiya, T. Suzuki, et al, Phys. Rev. B **68**, 155105 (2003).
- [36] M. Buron, E. Collet, M.H. Lemée-Cailleau, et al, in[7], p. 357; H. Okamoto, T. Koda, Y. Tokura et al, Phys. Rev. B **43**, 8224 (1991); S. Horiuchi, R. Kumai, Y. Okimoto et al, Phys. Rev. Lett. **85**, 5210 (2000).
- [37] J.-P. Pouget, S.K. Khanna, F. Denoyer, et al, Phys. Rev. Lett. **37**, 437 (1976).
- [38] S. Kagoshima, T. Ishiguro and H. Anzai, J. Phys. Soc. Japan, **41**, 2061 (1976).
- [39] V.J. Emery, Phys. Rev. Lett. **37**, 107 (1976).

- [40] J.-P. Pouget in Semiconductors and Semimetals, E.M. Conwell ed., (Academic, New York, 1988), v. **27**, p. 87.
- [41] S.K. Khanna, J.-P. Pouget, R. Comes et al, Phys. Rev. B, **21**, 486 (1980).
- [42] A. Andrieux, H.J. Schulz, D. Jérôme and K. Bechgaard, Phys. Rev. Lett. **43**, 227 (1979).
- [43] S. Huizinga, J. Kommandeur, G.A. Sawatzky, et al, Phys. Rev. B **19**, 4723 (1979).
- [44] H. Seo and H. Fukuyama, J. Phys. Soc. Japan **66**, 124 (1997); H. Seo, in [7], p. 205.
- [45] K. Hiraki and K. Kanoda, Phys. Rev. Lett. **80**, 4737 (1998).
- [46] V. Ilakovac, S. Ravy, A. Moradpour et al, Phys. Rev. B, **52**, 4108 (1995).
- [47] F. Nad, P. Monceau and J. Fabre, J. Physique IV, **9**, 361 (1999); F. Nad, P. Monceau C. Garcel et al, Phys. Rev. B **62**, 1753 (2000); J. Phys.: C, **12**, L435 (2000).
- [48] F. Nad, P. Monceau, L. Kaboub and J.M. Fabre, Europhys. Lett., **73**, 567 (2006).
- [49] P. Monceau et al, this volume.
- [50] F. Nad, P. Monceau, M. Nagasawa and T. Nacamura, in [8], p. 15.
- [51] S.S.P. Parkin, J.C. Scott, J. Thorance and E.M. Engler in [1], p. 1111;  
J. Thorance in [1], p.799
- [52] H. Alloul, in [8], p. 27.
- [53] P. Monceau and F. Nad in [10], p. 2121.
- [54] F. Nad and P. Monceau, J. Physique IV C2, **3**, 343 (1993).
- [55] F. Nad, P. Monceau and K. Bechgaard, Solid State Commun. **95**, 655 (1995).
- [56] S. Brazovskii in [2], p. 301; also **cond-mat**/0304076.
- [57] S. Brazovskii in [7], p. 149; also **cond-mat**/0306006.
- [58] S. Brazovskii and N. Kirova, JETP Letters **33**, 4 (1981); S. Brazovskii, N. Kirova and S.I. Matveenko, Sov. Phys. JETP **59**, 434 (1984).
- [59] M.J. Rice and E.J. Mele, Phys. Rev. Lett. **49**, 1455 (1982).
- [60] See reviews of this volume by D. Jérôme, A. Lebed, C. Sa de Melo, D. Podolsky et al.
- [61] R. Bruinsma and V.J. Emery, J. Physique C3, **44**, 1155 (1983).
- [62] L.D. Landau and E.M. Lifshitz, Electrodynamics of Continuous Media (Pergamon Press, Oxford, 1960).
- [63] S. Barisic and S. Brazovskii, in Recent Developments in Cond. Matt. Phys., D. Devreese ed. (Plenum Press N.Y. 1981) **1**, p. 142 (1981).

- [64] V.J. Emery, R. Bruinsma and S. Barisic, Phys. Rev. Lett. **48**, 1039 (1982).
- [65] I.E. Dzyaloshinskii and A.I. Larkin, Sov. Phys. JETP, **34**, 422 (1972).
- [66] A. Luther and V.J. Emery, Phys. Rev. Lett. **33**, 589 (1974).
- [67] V.J. Emery in Highly Conducting One-dimensional Solids (Plenum Press, NY 1979) p. 247.
- [68] S. Brazovskii, Synth. Met., **152**, 309 (2005).
- [69] M. Dumm, M. Abaker and M. Dressel, in [8], p. 55.
- [70] V. Ilakovac, S. Ravy, J.-P. Pouget, et al, Phys. Rev. B, **50**, 7136 (1994).
- [71] S. Brazovskii and N. Kirova, Sov. Sci. Reviews., Sect. A, I.M. Khalatnikov ed., v. **5** (Harwood Acad. Publ., 1984).
- [72] S. Brazovskii, N. Kirova and S.I. Matveenko, Sov. Phys. JETP, **59**, 434 (1984).
- [73] S. Brazovskii and N. Kirova, JETP Letters, **33**, 4 (1981).
- [74] L. Lauchlan, S. Etemad, T.-C. Chung, et al, Phys. Rev. B **24**, 3701 (1981).
- [75] I. Gontia, S.V. Frolov, M. Liess, et al, Phys. Rev. Lett., **82**, 4058 (1999).
- [76] F. Nad, P. Monceau, C. Carcel and J.M. Fabre, J. Phys.: C, **13**, L717 (2001).
- [77] T. Nakamura, J. Phys. Soc. Japan, **72**, 213 (2003).
- [78] K. Heuz, M. Fourmigu, P. Batail, et al, Adv. Mater., **15**, 1251 (2003).
- [79] J. Sólyom, Adv. Phys., **28**, 201 (1979).
- [80] A.O. Gogolin, A.A. Nersesyan and A.M. Tsvelik, Bosonization Approach to Strongly Correlated Systems (Cambridge Univ. Press, 1999).
- [81] C. Bourbonnais and R. Duprat, in [3], p. 3.
- [82] T. Giamarchi et al, in this volume, and in [3], p.23.
- [83] S. Mazumdar, in [5], p. 1317; R.T. Clay, S. Mazumdar and D.K. Campbell, Phys. Rev. B, **67**, 115121 (2003).
- [84] J. Riera and D. Poilblanc, Phys. Rev. B **63** 241102 (2001).
- [85] M.J. Rice, A.R. Bishop, J.A. Krumhansl et al, Phys. Rev. Lett., **36**, 432 (1976).
- [86] P. Auban-Senzier, D. Jérôme, C. Carcel et al, in [3], p. 41; B. Korin-Hamzić, E. Tafra, M. Basleti'c et al, Phys. Rev. B **73** 115102 (2006).
- [87] Yu.I. Latyshev, P. Monceau, S. Brazovski, et al, in [8], p. 197; and Phys. Rev. Lett. **95**, 266402 (2005); *ibid.*, **96**, 116402 (2006); S. Brazovskii, Yu.I. Latyshev, S.I. Matveenko et al, in [8], p. 77;

- [88] S. Brazovskii and S. Gordyunin , JETP Letters **31**, 371 (1980).
- [89] S. Teber et al: in [7]; J. Phys: C, **13**, 4015 (2001); *ibid.*, J. Phys: C, **14**, 7811 (2002).
- [90] V.Ya. Krivnov and A.A. Ovchinnikov, Sov. Phys. JETP, **63**, 414 (1986).
- [91] S. Brazovskii, **cond-mat**/0204147,0006355.
- [92] H. Fukuyama and H. Takayama in [11], p. 41.
- [93] V. Vescoli, L. Degiorgi, W. Henderson et al, Science **281**, 1181 (1998).
- [94] M. Dressel, A. Schwartz and G. Grüner, Phys. Rev. Lett. **77**, 398 (1996).
- [95] H. Kleinert and K. Maki, Phys. Rev. B **19**, 6238 (1979).
- [96] K. Maki in [11], p. 125.
- [97] F.H.L. Essler, F. Gebhard, and E. Jeckelmann, Phys. Rev. B **64**, 125119 (2001).
- [98] D. Controzzi, F.H.L. Essler, and A.M. Tsvelik, Phys. Rev. Lett. **86**, 680 (2001).
- [99] V. Vescoli et al., Solid State Comm., **111**, 507 (1999).
- [100] A. Schwartz, M. Dressel, G. Grüner, et al., Phys. Rev. B **58**, 1261 (1998).
- [101] N. Kirova and S. Brazovskii, Current Applied Physics, **4**, 473 (2004) and Thin Solid Films, **403**, 419 (2002). N. Kirova, S. Brazovskii and A.R. Bishop, Synthetic Metals, **100**, 29 (1999).
- [102] C. Jacobsen, D.B. Tanner and K. Bechgaard, Phys. Rev. B **28**, 7019 (1983); D. Pedron, R. Bozio, M. Meneghetti et al, Phys. Rev. B **49**, 10893 (1994).
- [103] M.J. Rice, Phys. Rev. Lett., **37**, 36 (1976).
- [104] M. Nagasawa, F. Nad, P. Monceau et al, in [3], p. 119.
- [105] W. Yu, F. Zhang, F. Zamborszky, et al, Phys. Rev. B **70**, 121101 (2005).
- [106] N. Kirova and S. Brazovskii, "Conjugated polymers at the verge of strongly correlated systems and 1D semiconductors", Synthetic Metals, **41**, 139 (2004).
- [107] S. Fujiyama and T. Nakamura, Phys. Rev. B **70**, 045102 (2004).
- [108] J. Tranquada in [7], p. 239. and refs. therein.
- [109] C. Bourbonnais and D. Jérôme in Adv. Synth. Met., (Elsevier 1999); **cond-mat**/9903101.
- [110] H.K. Ng, T. Timusk, and K. Bechgaard, Phys. Rev. B **30**, 5842 (1984); H.K. Ng, T. Timusk, D. Jérôme et al, Phys. Rev. B **32**, 8041 (1985); N. Cao, T. Timusk, and K. Bechgaard in [10], p. 1719.
- [111] B. Hennion, J.-P. Pouget and M. Sato, Phys. Rev. Lett., **68**, 2374 (1992) and *ibid.* **69**, 3266 (1992).

- [112] See articles in [11].
- [113] A. Finkelstein and S. Brazovskii, J. Phys. C, **14**, 847 (1981); and Solid State Commun., **38**, 745 (1981).
- [114] Y. Nogami, K. Oshima, K. Hiraki et al, J. Physique IV, **9**, 357 (1999); and Synth. Met., **102**, 1778 (1999).
- [115] L. Perfetti, H. Berger, A. Reggiani, et al, Phys. Rev. Lett. **87**, 216404 (2001); L. Perfetti, S. Mitrovic, G. Margaritondo, et al, Phys. Rev B **66**, 075107 (2002).
- [116] V. Shikin, Sov. Phys. Usp. Fiz. Nauk **158**, 127 (1989).
- [117] V.B. Preobrazhensky and A.N. Taldenkov, J. Physique IV C2, **3**, 57 (1993); V.B. Preobrazhensky, A.N. Taldenkov and V.V. Frolov, Synth Met., **55-57**, 2617 (1993).
- [118] G.X. Tessema, M.J. Skove and Y.T. Tseng, J. Physique IV C2, **3**, 53 (1993); J. Kuh, Y.T. Tseng, K. Wagner, et al, Phys. Rev. B **57**, 14576 (1998).
- [119] F. Zwick, S. Brown, G. Margaritondo et al, Phys. Rev. Lett. **79**, 3982 (1997).
- [120] F. Zwick, D. Jérôme, G. Margaritondo, et al, Phys. Rev. Lett., **81**, 2974 (1998).
- [121] J.-P. Pouget in [4], to be publ.
- [122] F. Nad, P Monceau, T. Nakamura et al, J. Phys.: C, **17**, L399, (2005); K. Furukawa, T. Hara and T. Nakamura, J. Phys. Soc. Japan, **74**, p. 3288 (2005).
- [123] D. Radic, A. Bjelis and D. Zanchi, Phys. Rev. B **69**, 014411 (2004); and in [8], p. 281.
- [124] S. Haddad et al, Phys. Rev. Lett., **51**, 89 (2002); and M. Heritier et al in this volume.
- [125] H.I. Ha, A.G. Lebed, and M.J. Naughton, Phys. Rev. B **73**, 033107 (2006).
- [126] S. Brazovskii and V. Yakovenko, Sov. Phys. JETP Letters **43** (1986) 134.

## A Earnshaw instability. Ion in the cage.

Empirically we see a systematic difference between the usual  $\vec{q} \neq 0$  anion ordering and the  $\vec{q} = 0$  ferroelectric transitions. The first ones are always observed for non-centrosymmetric anions, so that the orientational ordering was supposed to be a principle mechanism [61], with positional displacements being its consequences. The accent on the orientational ordering was probably one of reasons, why the hidden  $\vec{q} = 0$  transitions were not understood initially. Oppositely to  $\mathbf{q} \neq \mathbf{0}$  AOs, the  $\vec{q} = 0$  ones are mostly observed in systems with the non-centrosymmetric anions. Then we should think about a universal mechanism related only to the positional instability. This is apparently the case of the Earnshaw theorem [62], which states that a classical crystal with only Coulomb interactions is never stable. Our compounds may be regarded as such, as long as the cavity for the ion is large enough and they are allowed to move to minimize the Coulomb energy of the charge transfer. The Earnshaw instability will probably develop itself as a displacement  $\mathbf{u}$  towards one of the two closest molecules along the diagonal connecting

the nearest molecules on neighboring stacks, Fig. 3. Then in all cases, both centrosymmetric and non-centrosymmetric, there is a double well potential (or the potential is flattened [121] at least) for either displacements or orientations, or for both. It can also happen that for non-centrosymmetric ions, with orientation as another degree of freedom, new directions of  $\vec{u}$  are enforced. Then the former ones may be abandoned, what happens probably in the relaxed  $(\text{TMTSF})_2\text{ClO}_4$ <sup>14</sup>. Otherwise, the former displacive minima can be preserved which opens the possibility for a sequence of transitions of  $T_{\text{CO}}$  and  $T_{\text{AO}}$  types, as it was observed in case of  $(\text{TMTTF})_2\text{ReO}_4$ .

We suggest an elementary illustration of the purely ionic instability. Consider a single ion in the cage formed by four oppositely charged molecules from two neighboring stacks. Let  $a$  is the intramolecular spacing (stack period) and  $h$  is the distance from the ion to the stack. If we allow for the ion displacements  $\delta a$  along the stack, then the energy of Coulomb interactions will change as

$$\delta W \approx \frac{(h^2 - a^2/2)}{(h^2 + a^2/4)^{5/2}} (\delta a)^2$$

The system is unstable with respect to the longitudinal displacement  $\delta a$  if  $2h^2 < a^2$ . Otherwise, if  $2h^2 > a^2$ , it is unstable with respect to the transverse displacement  $\delta h$ . These two cases correspond to instabilities observed in  $(\text{TMTTF})_2\text{SCN}$  and  $(\text{TMTSF})_2\text{ClO}_4$ .

The quantitative criterium discriminating the types of instabilities may change if we improve calculations by taking into account the actual charge distribution over the large molecule, and their whole array. But the qualitative statement on the instability, the Earnshaw theorem, can be violated only by quantum mechanical effects like the orientational energy of methyl end groups forming the cage. Altogether, the double well potential for the ion will be formed.

These expectations give a sound interpretation of the very strong isotope effect upon deuteration [26, 122]. The  $T_{\text{CO}}$  enhancement can be caused [121] by the shortening of the (C-D) bonds, in comparison with the (C-H) ones, in methyl groups, thus widening the ion's cage and reducing its stability.

## B Permittivity sources.

### B.1 Estimations for the ionic contribution to $\varepsilon$ .

A purely ionic contribution near the  $\vec{q} = 0$  instability is expected to be

$$\varepsilon_i = 4\pi \frac{e^2}{\Omega} \frac{\partial u}{\partial eE} \sim 4\pi \frac{e^2}{a} \left(\frac{u_0}{a}\right)^2 \frac{1}{T_{\text{CO}}} \frac{T_{\text{CO}}}{T - T_{\text{CO}}} \sim 10^1 \frac{T_{\text{CO}}}{T - T_{\text{CO}}}$$

where  $\Omega$  is the unit cell volume,  $u_0 \sim 0.1a$  is a guess for the equilibrium displacement at low  $T$ , and also we have estimated  $\partial u / \partial eE \sim u_0^2 / T_{\text{CO}}$ . We see that the anomaly may develop upon the background value of only  $10^1$  which is 3 orders of magnitude below the experimental scale of  $\varepsilon \approx 2.5 \cdot 10^4 T_{\text{CO}} / |T - T_{\text{CO}}|$  [23].

---

<sup>14</sup>In this sense, the traditional interpretation of specifics of small anions as the "negative chemical pressure" should be revised. A small ion is allowed to realize larger varieties of its displacive instability [121], one of them fortunately gives rise to the  $\vec{q}_3$  structure favorable to superconductivity.

## B.2 Phase instability.

Consider the interference of ionic displacements and the charge ordering. Suppose the stability of the anionic system is controlled by a parameter  $K$  such that  $K = 0$  would correspond to the instability due to short range interactions of charges calculated without the contribution from electronic correlations. For homogeneous deformations and in presence of an external electric field  $E$ , the energy per stack reads

$$\frac{1}{\pi}E\varphi - U_b \cos 2\varphi - U_s \sin 2\varphi + \frac{K}{2}U_s^2 \quad (10)$$

For shortness we do not distinguish bare and renormalized values. Expanding in small  $\varphi$ , the minimization yields

$$U_s = \frac{E/2\pi}{U_b K - 1}, \quad \varphi = -\frac{E/\pi}{U_b - K^{-1}}, \quad \varepsilon = \frac{4e\varphi}{sE} = \frac{4e^2/\pi s}{U_b - K^{-1}}$$

We see that the transition of a joint electron-ion instability takes place at  $K = U_b^{-1}$ , well above the point  $K = 0$  of a purely ionic one.

To keep nonlinearity at hand and to access the new ground state below the instability, we should exclude from (10) only  $U_s$  to arrive at the energy (for  $E = 0$ )

$$F(\varphi) = -U_b \cos 2\varphi + \frac{1}{2K} \cos^2 2\varphi + \text{const}$$

At  $U_b > K^{-1}$  there is only one minima at  $\varphi = 0$  but at  $U_b = K^{-1}$  this point becomes unstable which originates the anomaly in  $\varepsilon$ . At  $U_b < K^{-1}$  the two new minima appear at  $\varphi = \pm\alpha$  (first closely, with  $\alpha \approx \sqrt{(1 - KU_b)/2}$ ) which makes the chain to be polarized.

## C Competing philosophies for organic conductors.

Since long time, there are two opposing philosophies for interpretations of these magnificent materials:

A. *Generic picture* summarized in [109] implies that the sequence of electronic phases follows a smooth variation of basic parameters reducible to the effective pressure, see Fig. 5 in [109]. The majority of compounds with non-centrosymmetric anions were abandoned, presumably their AOs were thought to exhort ill defined or undesirable complications.

The advantages are appealing:

- a) Concentration on simplest examples avoiding structural effects;
- b) Generality in a common frame of strongly correlated systems driven mostly by basic parameters - interactions versus the bandwidth;
- c) Extensive use of experiments under pressure.

But there is also another side of the coin:

- 1) Concentration on only simplest examples avoiding the rich information [15] on correlation of electronic and structural properties;
- 2) Necessity to introduce the case of the non-centrosymmetric anion  $\text{ClO}_4$  to demonstrate the appearance of the superconductivity without pressure.<sup>15</sup>;

---

<sup>15</sup>The logic of the "effective pressure" demands to show for this compound only the quenched phase with the SDW state, rather than the relaxed phase where the superconductivity appears only after the particular structural transition of the AO.

- 3) Accent upon pressure as a universal parameter;
- 4) Ignoring the ‘structureless’ transition’, which are typical just for these selected compounds with centrosymmetric anions; hence loosing the dominating effect of the CO/FE.

*B. Specific picture* developed in [17, 126, 18, 63] suggested the synergy of structural and electronic phase transitions with the accent upon compounds with AOs. It extends naturally to new observations on charge ordering and ferroelectricity. Its main statements are the following (see [17] and Ch.6 of [18] for applications):

- a) Displacive, rather than orientational, mechanisms are driving the AOs (the Earnshaw instability of separated charges);
- b) Each fine structural change exerts a symmetrically defined effect which triggers a particular electronic state;
- c) 1D ”g-ological” phase diagram results in 2D, 3D phase transitions only when it is endorsed by appropriate symmetry lowering effects;
- d) Main proof for the 1D physics of the Mott transitions is given by the  $\vec{q}_2$  structure of the (TMTTF)<sub>2</sub>SCN. (Today it is seen as the AFE case of the CO.)
- e) Superconductivity appears only if the system is drawn away from the half filling thus avoiding the Mott insulator state. It happens in the relaxed phase of the (TMTSF)<sub>2</sub>ClO<sub>4</sub> thanks to the unique  $\vec{q}_3$  type of the anion ordering leading to inequivalence (CD in today’s terms) of chains<sup>16</sup>

But there are difficulties of this picture as well.

1. In applications to *Se* compounds there are common problems of any quasi 1D approach confronting the success of the band picture for the FISDWs (and vice versa!).
2. There are cases of the superconducting state without observation of the particular  $\vec{q}_3$  type of the AO.<sup>17</sup>
3. Missing opportunity to view the anion ordering transition in (TMTTF)<sub>2</sub>SCN case as the AFE charge ordering.
4. Unawareness of the later discovered structureless transitions.

## D History Excursions.

Correlation between electronic phases and fine structural effects of the AOs has been noticed [63, 17, 18] and exploited in details [17, 18] long time ago. Experiments generally prove this correlation but also demonstrated deviations, see [15], from the unique correspondence suggested at the earlier stage. The discrepancies are related to the third variable ingredient: the electronic dispersion in the interchain direction. The recent events call again for a unifying picture of electronic and structural effects which returns us to suggestions already made two decades ago. Below we quote from ill known publications written in early-mid 80’, whose views become relevant nowadays.

**Extracts from [17].** For more details and applications see Ch.6 in [18].

---

<sup>16</sup>This is a purely defined case of what today is called the ”internal doping”. Estimations for its magnitude, i.e. the potential  $\pm W$  of the interchain charge disproportionation, range from moderate  $W \approx 50K$  [124, 125] to high  $W \approx 250K$  [123] and even higher [126] values. The uncertainty comes from different interpretation of the fast oscillations.

<sup>17</sup>Nevertheless, the recent views on independent AOs allows to suggest that the  $\vec{q}_3$  structure is still there, at least in local or dynamic form without the long range order. Low  $T$  structural studies under pressure, of particularly (TMTSF)<sub>2</sub>PF<sub>6</sub>, are required.



... This theory permits us to suggest a general model for the phase diagram of the Bechgaard salts in a way that the variation of electronic states is mainly determined by the crystal symmetry changes.

... 1D divergent susceptibilities give rise to observable phenomena only if the pair coherence is preserved in the course of the interchain tunneling. In the gapless regime it can be maintained by proper interchain electronic phase shifts which can appear due to some symmetry changes.

... Experimental data show us the following correlation between the anionic structure (characterized by the wave vector  $\vec{q}$ ) and the state of the electronic system.<sup>18</sup>

1. Unperturbed structure. Bonds are dimerized. PD: M→MI→SDW.  
The last two phases are clearly separated only in TMTTF subfamily.
2.  $\vec{q}_2 = (0, 1/2, 1/2)$ . The molecules are not equivalent. PD: M→MI→SDW (or CDW = Spin-Peierls).  $T_{\text{MI}}$  and  $T_{\text{SDW}}$  are well separated  
(X = SCN:  $T_{\text{MI}} = 160K$ , while  $T_{\text{SDW}} = 7K$ )
3.  $\vec{q}_3 = (0, 1/2, 0)$ . The neighboring stacks are not equivalent.  
PD: M→SC→FISDW.
4.  $\vec{q}_4 = (1/2, 1/2, 1/2)$ . The tetramerization.  
PD: M→I transition being driven externally by the AO.

... The rare case 2. helps us to fix the model for the whole family: a strongly correlated 1D state with the separation of charge- and spin degrees of freedom. The typical case 1. qualitatively corresponds to the same model while the separation is less pronounced and interpretation may be controversial.<sup>19</sup>

The most important for appearance of the SC is the case 3.: the alternating potentials lead to some redistribution of the charge between the two types of stacks, hence the system is driven from the two fold commensurability which removes the Umklapp scattering, destroys the Mott-Hubbard effect and stabilizes the conducting state down to lower temperatures where the SC can appear.<sup>20</sup>

### Extracts from [63].

Here are some extracts from [63]<sup>21</sup>, which itself was an extension of earlier observations on effects of counterions in charge transfer CDWs of the KCP type [88]. A better known later publication is [64].

...We propose an alternative explanation of  $(\text{TMTSF})_2\text{PF}_6$ , based on the fact that this material possesses a weak dimerization gap  $\Delta$ . This gap is due to the environment of the given chain, which, unlike the chain itself, does not possess a screw symmetry along the chain axis. Without the effect of the environment the band is quarter-filled. The environment ( $\text{PF}_6$ , etc.) opens a

---

<sup>18</sup>Additional notations here: PD - phase diagram, MI - magnetic/Mott insulator.

<sup>19</sup>Fortunately it is unambiguous today, two decades later.

<sup>20</sup>This is a clear case of the "internal doping" in today's terminology.

<sup>21</sup>[63] was probably the first theoretical work performed in response to the discovery of the organic superconductivity within first weeks. Hence it speaks only about the case of X=PF<sub>6</sub>: the zero pressure superconductor X=ClO<sub>4</sub> was not discovered yet.

small gap  $\Delta$  in the middle of this band, which therefore becomes half-filled. Hence also small are the corresponding constant for the Umklapp scattering:  $g_3 \sim g_1 \Delta / E_F$ . The effect of  $g_3$  appears only below sufficiently low temperature  $T_3 \sim E_F g^{1/2} (g_3/g)^{1/g}$ ,  $g = 2g_2 - g_1$ .

... Assuming the pressure suppresses  $g_3$  and with it  $T_3$ , the Josephson coupling  $J$  of superconducting fluctuation will finally overcome the Umklapp scattering. This interpretation explains the observations in  $(\text{TMTSF})_2\text{PF}_6$  as a result of competition of the two small (off-chain) parameters,  $g_3$  and  $J$ , rather than as a result of the accidental cancelation of the large coupling constants  $2g_2$  and  $g_1$  (D. Jerome and H. Schulz, Adv. in Physics **31**, 299 (1982)).

... In this way there appears a region in the phase diagram where the superconductivity exists in absence of  $g_3$ , but where the CDW is introduced by  $g_3$ .

... A closer examination of the model shows that it is the triplet<sup>22</sup> superconductivity.

---

<sup>22</sup>This proposal, apparent from already existing by that old time theories - see e.g. [79], is back to the agenda today, 25 years later.